

RAUNO LUST

Bioelectrochemical systems for
enhanced removal of nitrate from water
with a low electron donor concentration



DISSERTATIONES TECHNOLOGIAE CIRCUMIECTORUM
UNIVERSITATIS TARTUENSIS

36

RAUNO LUST

Bioelectrochemical systems for
enhanced removal of nitrate from water
with a low electron donor concentration



Department of Geography, Institute of Ecology and Earth Sciences, Faculty of Science and Technology, University of Tartu, Estonia.

This dissertation has been accepted for the commencement of the degree of Doctor of Philosophy in Environmental Technology at the University of Tartu on 6 June 2022, by the Scientific Council on Environmental Technology, Faculty of Science and Technology, University of Tartu.

Supervisors: Prof. Ülo Mander
Institute of Ecology and Earth Sciences
University of Tartu, Estonia

Associate Prof. Kuno Kasak
Institute of Ecology and Earth Sciences
University of Tartu, Estonia

Associate Prof. Jaak Nerut
Institute of Chemistry
University of Tartu, Estonia

Opponent: Dr Carlos Alberto Arias
Senior Researcher
Department of Biology – Aquatic Biology
Aarhus University, Denmark

Commencement: University of Tartu, Vanemuise 46-327, Tartu, at 10:15 on 31 August 2022.

Publication of this dissertation is granted by the Institute of Ecology and Earth Sciences, University of Tartu.



European Union
European Structural
and Investment Funds



Investing
in your future

ISSN 1736-3349
ISBN 978-9949-03-931-9 (print)
ISBN 978-9949-03-932-6 (pdf)

Copyright: Rauno Lust, 2022

University of Tartu Press
www.tyk.ee

CONTENTS

ORIGINAL PUBLICATIONS.....	6
ABBREVIATIONS AND ACRONYMS	7
ABSTRACT	9
1. INTRODUCTION.....	11
2. MATERIALS AND METHODS (Articles I–IV)	14
2.1. Site description and sampling (Article I)	14
2.2. Reactor design (Articles II & III).....	15
2.3. Inoculum and synthetic wastewater characteristics (Articles II & III)..	17
2.4. Operating conditions in a two-chamber reactor (Article II).....	17
2.5. Operating conditions in a single chamber reactor (Article III)	18
2.6. Chemical analysis (Articles I–III).....	22
2.7. Gas analysis (Article II)	22
2.8. Quantitative Polymerase Chain Reaction (Article III).....	23
2.9. Calculation of the nitrate removal rate and the Faradaic efficiency (Article III).....	24
2.10. Statistical analysis (Articles I & II).....	25
2.11. Bibliometric analysis related to microbial fuel cell in constructed wetland (Article IV).....	25
3. RESULTS AND DISCUSSION	26
3.1. Diffuse contamination of groundwater with nitrate and its mitigation on to constructed wetlands in agricultural catchments (Article I)	26
3.2. Optimization of reactor design in experimental systems (Articles II & III)	27
3.3. Optimization of operating conditions in experimental systems (Article III).....	34
3.4. Changes in nitrogen-related functional genes in microbial electrosynthesis reactor (Article III)	36
3.5. Greenhouse gas fluxes in microbial electrosynthesis reactor (Article II)	37
3.6. Bibliometric analysis related to microbial fuel cell in constructed wetland (Article IV).....	38
3.7. Synthesis of 3.1–3.6.....	40
4. CONCLUSIONS.....	44
REFERENCES.....	45
SUMMARY IN ESTONIAN	50
ACKNOWLEDGEMENTS	55
PUBLICATIONS	57
CURRICULUM VITAE	139
ELULOOKIRJELDUS.....	141

ORIGINAL PUBLICATIONS

This thesis is based on the following publications, which are referred to in the text with Roman numerals. Published papers are reproduced in print with the permission of the publisher.

- I. Kill, K., Pärn, J., **Lust, R.**, Mander, Ü., Kasak, K., 2018. Treatment efficiency of diffuse agricultural pollution with constructed wetland impacted by groundwater seepage. *Water* 10, 1601.
<https://doi.org/10.3390/w10111601>
- II. **Lust, R.**, Nerut, J., Kasak, K., Mander, Ü. 2020. Enhancing nitrate removal from waters with low organic carbon concentration using bioelectrochemical systems – a pilot-scale study. *Water* 12, 516.
<https://doi.org/10.3390/w12020516>
- III. **Lust, R.**, Nerut, J., Gadegaonkar, S., Kasak, K., Espenberg, M., Visnapuu, T., Mander, Ü., 2022. Single-chamber microbial electrosynthesis reactor for nitrate reduction from waters with a low electron donors concentrations: from design and set-up to the optimal operating potential. *Sent to Frontiers in Environmental Science*, under review.
- IV. Ji, B., Zhao, Y., Vymazal, J., Mander, Ü., **Lust, R.**, Tang, C. 2021. Mapping the field of constructed wetland-microbial fuel cell: A review and bibliometric analysis. *Chemosphere* 262, 128366.
<https://doi.org/10.1016/j.chemosphere.2020.128366>

Author's contribution to the articles: '*' denotes a minor contribution, '**' denotes a moderate contribution, '***' denotes a major contribution.

Categories	Author's contribution			
	I	II	III	IV
Original idea	*	***	***	*
Study design	*	***	***	*
Data processing and analysis	**	***	***	*
Interpretation of the results	*	***	***	**
Writing the manuscript	*	***	***	*

ABBREVIATIONS AND ACRONYMS

AEM	anion exchange membrane
amoA	ammonia monooxygenase, a gene that oxidates ammonia to hydroxylamine (NH ₂ OH)
Anammox	anaerobic ammonium oxidation, a process by which bacteria transforms ammonium and nitrogen dioxide into nitrogen gas and water
BES	bioelectrochemical system
CE	counter electrode
CH₂O	formaldehyde, methanal
CH₄	methane
Cl⁻	chlorine ion
CO₂	carbon dioxide
COD	chemical oxygen demand
Comammox	complete ammonia oxidation, a name added to an organism that can oxidate ammonia to nitrite and then into nitrate through the process of nitrification
CV	cyclic voltammetry
CW	constructed wetland
CW-MFC	constructed wetland – microbial fuel cell
DNA	deoxyribonucleic acid
DNRA	dissimilatory nitrate reduction to ammonia
DO	dissolved oxygen
EC	electric conductivity
EIS	electrochemical impedance spectroscopy
FWS CW	free water surface constructed wetland
GHG	greenhouse gas
GSA	geometric surface area
H₂	hydrogen
H₂O	water
HCl	hydrogen chloride
KNO₃	potassium nitrate
MES	microbial electrosynthesis
MESR	microbial electrosynthesis reactor
MFC	microbial fuel cell
N₂	nitrogen
N₂O	nitrous oxide

NaOH	sodium hydroxide
NH₄⁺	ammonium ion
nirK	nitrite reductase, a gene that reduces nitrite to nitrous oxide
nirS	nitrite reductase, a gene that reduces nitrite to nitrous oxide
NO₂⁻	nitrite ion
NO₃⁻	nitrate ion
nosZI	nitrous oxide reductase, a gene that reduces nitrous oxide to nitrogen
N₂	nitrogen
O₂	oxygen
OCP	open circuit potential
PEM	proton exchange membrane
qPCR	quantitative polymerase chain reaction
RE	reference electrode
SCE	saturated calomel electrode
SHE	standard hydrogen electrode
SO₄²⁻	sulphate ion
TC	total carbon
TIC	total inorganic carbon
TN	total nitrogen
TOC	total organic carbon
WE	working electrode

ABSTRACT

Diffuse agricultural pollution and the discharge of untreated wastewater degrades water quality in surface and groundwater globally. Constructed wetlands (CW) can be used to treat surface water to improve water quality. However, one problematic pollutant is nitrate (NO_3^-), the removal efficiency of which is typically hindered by the low concentration of electron donors. They are necessary for denitrifying microorganisms that use electrons to reduce NO_3^- to nitrogen. The same problem occurred in Vända CW, where the NO_3^- removal efficiency was -31.6% , meaning that the concentration of NO_3^- increased while passing through the system. This was caused by a combination of two aspects: the intrusion of NO_3^- rich groundwater and the low NO_3^- removal rate. The microbial electro-synthesis reactor (MESR) was thought to be a possible solution to enhance the denitrification and therefore increase NO_3^- removal efficiency in the CW. It is a bioelectrochemical system where the working electrode (WE) is used to supply microorganisms with electrons by applying electricity.

At first, a two-chamber MESR was constructed and operated at a WE potential of -306 mV vs a standard hydrogen electrode (SHE) for 38 days and thereafter it was inoculated with sludge taken from a municipal wastewater treatment plant. A study showed that the MESR was able to increase the NO_3^- removal rate from 0.7 to 1.4 $\text{mgN-NO}_3^-/(\text{L} \times \text{day})$ for the MESR and the control reactor, respectively. At the same time, the average nitrous oxide emission was smaller in the MESR -0.64 compared to the control reactor's -0.01 $\text{mgN}/(\text{m}^2 \times \text{h})$. Despite the increase in NO_3^- removal efficiency, the increase itself was too small. The use of a two-chamber MESR was able to retain the oxygen produced on the counter electrode (CE) away from WE chamber; however, it also caused problems with pH, which needed to be regulated constantly.

A second attempt was made with a single-chamber MESR. To keep oxygen production on the CE as low as possible, an outer electrode was used as the CE, because compared to the inner electrode it had a larger geometric surface area. Using the single-chamber MESR, the pH remained stable at around 7.3. Several WE potentials were tested during the experiment, and at the potential of -756 mV vs SHE, the concentration of NO_3^- started to reduce significantly. In the control reactor, however, the NO_3^- concentration did not change until the end of the first experimental cycle (208 days). The optimal potential was found to be -656 mV vs SHE, where the NO_3^- removal rate was 3.8 ± 1.2 $\text{mgN-NO}_3^-/(\text{L} \times \text{day})$. Compared to the CE, the abundance of nitrite reductase and nitrous oxide reductase genes were significantly higher on the WE, indicating that the NO_3^- reduction was driven by denitrification. At the WE potential of -756 mV vs SHE, an increase in ammonium (NH_4^+) concentration was observed, meaning that at lower WE potentials the dissimilatory nitrate reduction to ammonium can also compete with denitrification. However, at higher WE potentials, the MESR was able to remove NH_4^+ and no intermediate compounds related to denitrification accumulated. Therefore, it is very important to choose the right WE potential when working with the MESR.

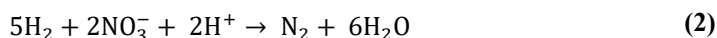
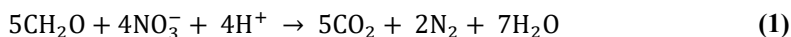
Based on the NO_3^- removal rate achieved with the MESR experiment, the WE's geometric surface area should be *ca* 964 m^2 in the Vända CW. Since there is a problem with groundwater seepage, the MESR should be placed near the outlet. Based on the calculations, the last section of the CW is large enough to accommodate the MESR. The current output of the current source must be at least 434 A to ensure that sufficient power is available. However, before implementing the MESR on such a large scale, it would be wise to conduct some pilot scale studies to evaluate different electrode configurations and assess how the flow rate and lower water temperatures affect the NO_3^- removal rate.

As the MESR requires energy to remove NO_3^- , a literature analysis was conducted to see the currently researched topics related to constructed wetland – microbial fuel cells. Key term occurrences showed that the main groups of topics were related to ‘bioelectricity generation performance’, ‘microbial studies’, ‘removal of problematic pollutants’ and ‘removal performance of traditional contaminants’. With time, the research topics have become more specific and are more focused on different plants, substrates, electrode materials, hydraulic regimes and cell structures and how they affect purification efficiency and power generation. However, the current constructed wetland – microbial fuel cell (CW-MFC) systems are in the pilot stage or lab-scale, and no articles were found where a CW-MFC could be used for NO_3^- removal in the absence of electron donors.

1. INTRODUCTION

Nitrogen emission to the environment from intensive farming, excessive use of fertilizers and the discharge of untreated wastewater is causing diffused surface and groundwater pollution globally [1,2]. In surface water, high nitrate (NO_3^-) concentration is causing eutrophication, which can lead to a loss of biodiversity [3]. Assessments show that in many countries, including Portugal, Iran and France, NO_3^- concentration in groundwater exceeds the $50 \text{ mgNO}_3^-/\text{L}$ threshold [4–7]. At NO_3^- concentration exceeding $50 \text{ mgNO}_3^-/\text{L}$, the water is categorized as unsafe for drinking by the World Health Organization because consumption of NO_3^- in larger amounts can cause methemoglobinemia or play a potential role in the development of digestive tract cancer [1,3]. Therefore, it is essential to develop technology to remove NO_3^- from water.

Depending on the characteristic of the water being treated, the structure and operating practices of water treatment systems can vary considerably. Constructed wetlands (CW) have been used for treating nitrogen rich waters, where pollutants are removed by vegetation and microbial processes [8,9]. In most cases, nitrogen is removed from water by utilizing various microbes that conduct different microbial processes, for example nitrification, denitrification and anaerobic ammonium oxidation [8]. In this thesis, the focus is on denitrification – a process whereby NO_3^- is turned into nitrogen (N_2) [10]. This can happen via heterotrophic or autotrophic pathways, depending on the compounds and the bacteria available in the environment [11]. In heterotrophic denitrification (1), microbes use organic compounds as electron donors and carbon sources [12]. In autotrophic denitrification (2), the microbes use sulphur, ferrous iron, hydrogen (H_2) or other inorganic compounds as electron donors and inorganic carbon, such as carbon dioxide (CO_2) or carbonate, as carbon sources for growth [12].



Low concentration of electron donors is one of the main aspects that hinders denitrification [13]. If the concentration of electron donors is low, intermediate compounds, such as nitrite (NO_2^-) or nitrous oxide (N_2O), will start to accumulate [13]. With NO_2^- accumulation, denitrification can be inhibited and N_2O is a greenhouse gas known to cause climate warming. To make sure that water purification via denitrification works optimally, and that the impact on the climate is low, it is essential to provide sufficient electron donors to the system. Often, organic carbon, in the form of methanol or ethanol, is added to the system to provide an organic source for microorganisms in wastewater treatment plants [14,15]. In CWs, wood-mulch, activated carbon or biochar is used as an additional source of organic carbon [16]. Providing the system with additional organic carbon helps with NO_3^- removal. However, this approach cannot be used in every case. For example, addition of organic carbon to treat groundwater can cause secondary pollution.

For a while, microbial fuel cells (MFC) have been used to harvest energy (Figure 1) and increase the removal efficiency simultaneously [17]. Although, in cases where the electron donor concentration in the treatable water is low, MFCs have not shown any significant results in removing NO_3^- . As a result, another approach is necessary. Recent studies have demonstrated that some microorganisms i.e., *Geobacter* species, can acquire electrons provided by electrodes and use those electrons to reduce NO_3^- [18]. Therefore, instead of producing electricity in an MFC, the bioelectrochemical system (BES) can be used to enforce unspontaneous reactions by applying electricity. These systems are called microbial electrosynthesis cells (MES) (Figure 1). Many studies have been conducted to evaluate the possibility of performing various processes and to optimize reactor design, inoculation and operating practices [19–22]. Additional research has been conducted to describe the mechanisms of interaction between the microbe and the electrode, but the technology has not yet reached wide usage [23,24].

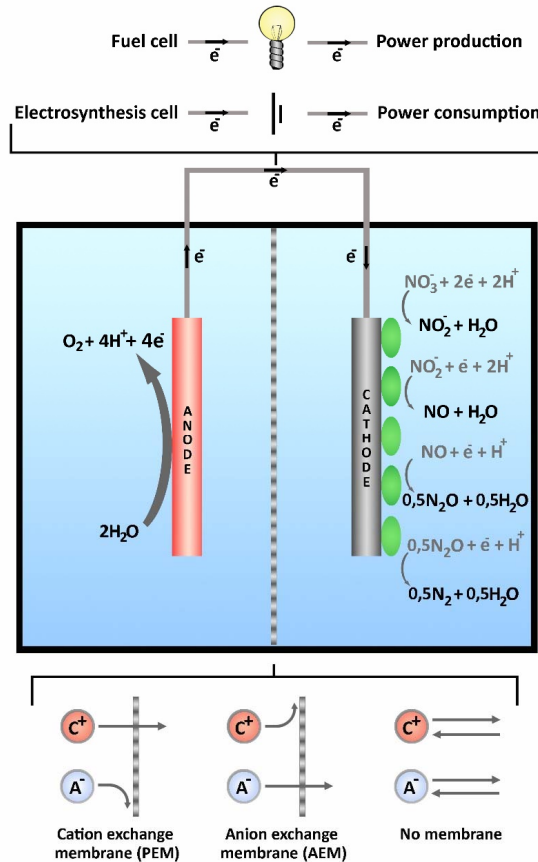


Figure 1. A basic set-up of a bioelectrochemical system, where water is oxidized on an abiotic anode and NO_3^- is reduced by a biocathode via autotrophic denitrification. The electrodes can be separated by a membrane to process two different types of electrolytes. Different types of membranes are shown at the bottom. The flow direction of electrons when it is operated as an electrosynthesis cell is shown on the wire and different external circuit options are shown on top. Four-step autotrophic denitrification is shown on biocathode.

Substitution of microorganisms' demand for electron donors with electrons provided via the electrode to enforce the NO_3^- removal in water has huge potential to overcome the previously mentioned environmental problems. If this technology were applicable on larger scale, it would help to overcome the main problem related to NO_3^- removal: the low electron donor to nitrogen ratio. Therefore, it is important to investigate this technology in more detail. The goals for this thesis were to:

- Achieve stable NO_3^- reduction by denitrification in the microbial electro-synthesis reactor (MESR) (Articles II & III);
- Find the optimal working electrode potential, where Faradaic efficiency is highest and no ammonium (NH_4^+) or intermediate compounds related to denitrification accumulate (Article III);
- Determine the effect of using a MESR on greenhouse gas (GHG) emissions (Article II);
- Understand how the use of electrodes affects the abundance of nitrogen-cycle-related functional genes (Article III);
- Evaluate the efficiency of an in-stream free water surface constructed wetland (FWS CW) to reduce diffuse agricultural pollution in the northern climate (Article I) and evaluate the possibility to integrate the MESR with the CW;
- Determine whether there has been an article released about CW-MFC, where it would have been used to reduce NO_3^- from water with a low electron donor (Article IV).

Hypotheses

It was hypothesized that:

1. The MESR can be used to provide electrons directly to microorganisms to substitute the electron donors;
2. Denitrification efficiency is influenced by the working electrode potential;
3. The MESR can be used to remove NO_3^- from water with a low organic carbon concentration.

2. MATERIALS AND METHODS (Articles I-IV)

2.1. Site description and sampling (Article I)

To understand the ability of FWS CWs to reduce nitrogen, an experiment at Vända FWS CW (58°17' N, 26°43' E) was carried out. The CW is located in the 2.2 km² Vända sub-catchment, which is part of the 258 km² Porijõgi River catchment in South-eastern Estonia. A figure where the study site location with the catchment area can be found in previously published article [25]. Approximately 62% of the Vända sub-catchment is intensively managed arable land. The region experiences a temperate climate, with four near-equal-length seasons. The growing season typically extends from late April to September. The mean annual air temperature is 6.3 °C and the mean annual precipitation is 726 mm, recorded at the nearby Tartu Observatory weather station in Tõravere.

For decades, both surface water and groundwater in the Vända sub-catchment have been impacted by the nutrient runoff and leaching from surrounding agricultural fields. Until 2015, when Vända FWS CW was established, no water protection measures had been used to control or reduce diffuse pollution [2,26]. The Vända FWS CW consists of two shallow water wetlands with a total area of around 0.4 ha (Figure 2), which is approximately 0.5% of the upstream catchment area. Due to its location in a valley, the CW is highly impacted by groundwater seepage since no specific insulation materials such as geomembrane or clay were used. To observe the NO₃ – N concentration in the groundwater, 10 piezometers (P1–P10, Figure 2) were installed, on the banks of the stream connecting the two wetlands. Previous grab sampling occasions have shown that this is the area where most of the groundwater from surrounding fields enters the system and which was therefore selected for monitoring[27].

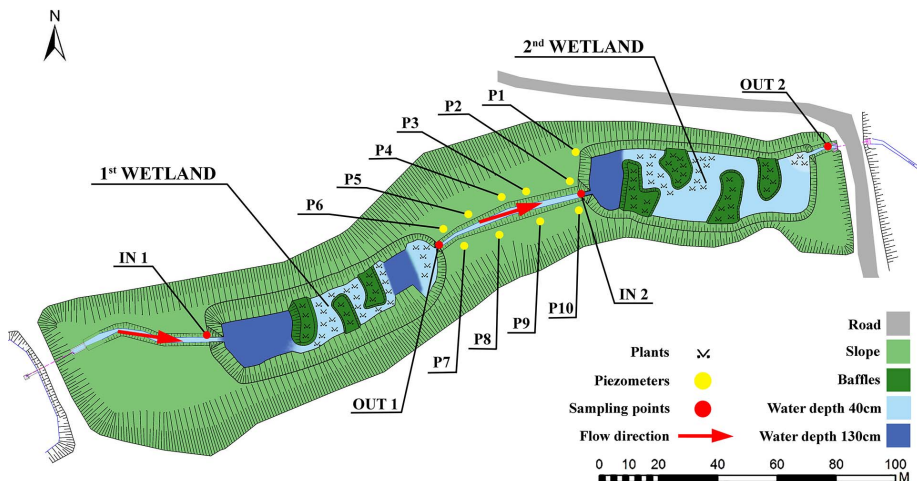


Figure 2. Layout of the Vända free water surface constructed wetland system capturing runoff from 2.2 km² catchment area.

Water samples were collected biweekly from March 2017, with a total of 132 samples taken during the study period. Each time, the samples were collected from the inlet (in 1 and in 2) and outlet (out 1 and out 2) of both CWs (Figure 2) and on a monthly basis from piezometers P1–P10.

2.2. Reactor design (Articles II & III)

To evaluate the possibility of using a MESR to remove NO_3^- from water with a low electron donor concentration, reactors made of Plexiglas with a total volume of 5.86 L (Figure 3) were used. The reactors were operated as three-electrode systems and were equipped with a reference electrode (RE).

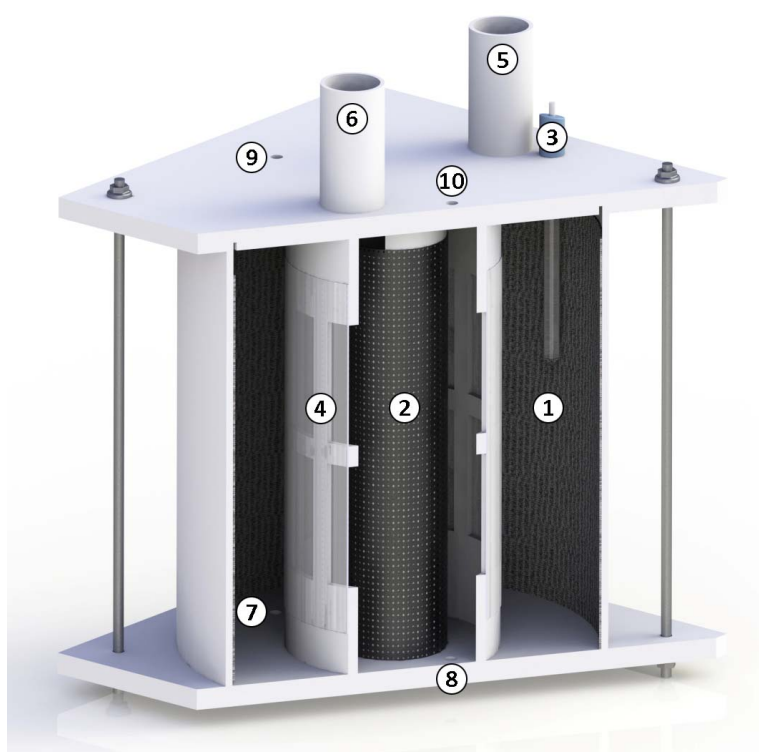


Figure 3. Reactor scheme: 1 – outer electrode; 2 – inner electrode; 3 – reference electrode; 4 – proton exchange membrane; 5, 6 – sampling ports of outer and inner chambers; 7, 8 – outer and inner chambers electrolyte inlets; 9, 10 – outer and inner chambers electrolyte outlets.

At first (Article II), the reactor was configured as a two-chamber reactor where the counter electrode (CE) chamber (inner chamber) with a volume of 1.37 L was separated from working electrode (WE) chamber (outer chamber) with a volume of 4.49 L by a *Nafion 117* proton exchange membrane (PEM). A two-chamber reactor was used because during the electrolysis, oxygen (O_2) is being produced on the CE and that O_2 can inhibit the denitrification process. The *Nafion 117* membrane was treated in a solution of hydrogen peroxide and boiled in 0.5 M sulphuric acid solution prior to each measurement series. WE 20×61 cm was made of carbon cloth (Figure 4.A) and CE (Figure 4.B) 20×16 cm was made of steel mesh (SS321 Grade, #20 Mesh, The Mesh Company, United Kingdom), which was covered with 1 mg/cm² carbon powder (Vulcan XC72R). Two pumps were used to mix electrolyte in both chambers. Both chambers also had openings for gathering gas and water samples (Figure 3).

During the first experiment, the pH did not remain neutral and so, for the second experiment (Article III), the reactor was configured as a single chamber reactor. For that, the PEM with the carrier module (Figure 3) was removed. To suppress O_2 production on the CE, the outer electrode with a much larger geometric surface area (GSA) was used as the CE, and the inner electrode was used as the WE. During the first experiment, there was a problem with the CE being corroded, therefore 3-mm thick graphite felt (Graphite felt PGF 3x1.200 m, CGT Carbon GmbH, Asbach, Germany) was used to prepare the CE and the WE (Figure 4.C), which had GSAs of 930 cm² and 255 cm², respectively. The electrode contacts were made from Grade-1 titanium wire with a cross section of 0.2 mm (Grade-1 Titanium Round Wire 0.2 mm x 50 m, Metal Clays 4 You, Mayfield, UK). Since graphite felt is a relatively brittle material, an electrically conductive glue was used during the second MESR experiment (Article III) to ensure proper contact between the graphite and the titanium. The glue was made from a graphite-based paint (Electric paint, Bare Conductive, London, UK) mixed with epoxy (Moment 5-minute repair Epoxy, Henkel AG, & Co. KGaA, Düsseldorf, Germany) in the ratio of 1 to 1.

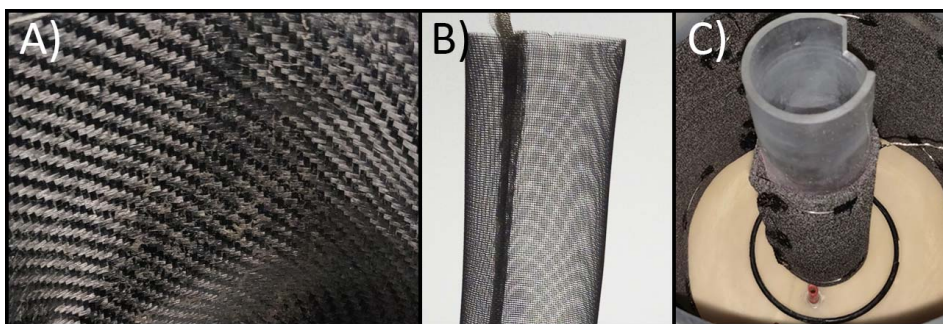


Figure 4. A) & B) Pictures of the working electrode (WE) and the counter electrode (CE; Article II), respectively. C) Picture of the WE and CE made of graphite felt (Article III)

2.3. Inoculum and synthetic wastewater characteristics (Articles II & III)

For the first MESR experiment (Article II), the activated sludge was taken from a basin of Tartu municipal wastewater treatment plant, where Anammox and denitrification processes are performed. The collected sludge was then centrifuged with a relative centrifugal force of 3550 G for 10 minutes to separate the sludge from the wastewater. 40 g of pre-treated sludge was added to the WE chamber as an inoculum.

During the first experiment, the NO_3^- removal rate was lower than generally reported in literature, and the lack of electroactive bacteria was considered one of the possible reasons. In many articles, the abundance of *Thiobacillus denitrificans* was found to increase during the experiments [28–30]. *Thiobacillus denitrificans* also have all the genes necessary for proceeding denitrification [31]. Because of that, an actively growing culture of *Thiobacillus denitrificans* was ordered from the DSMZ (German Collection of Microorganisms and Cell Cultures GmbH, Leibniz Institute, Brunswick, Germany) and used as an inoculum during the second experiment (Article III). The culture was cultivated, as instructed by the supplier in medium 113 (German Collection of Microorganisms and Cell Cultures GmbH, Leibniz Institute, Brunswick, Germany). The cultivation was conducted in three stages. First 5 mL of the culture was cultivated in a 25 mL medium. After three days, the inoculum was diluted by adding 270 mL of fresh medium. Thirty days later, the inoculum was further diluted by adding 200 mL of medium. Ten days later, the inoculum was stirred, and 200 mL of inoculum was used for each reactor (Reactor 1 and 2). To ensure that there were enough trace elements, 20 mL of trace element solution SL-4, described in medium 14 (German Collection of Microorganisms and Cell Cultures GmbH, Leibniz Institute, Brunswick, Germany), was also added to the reactor.

For both experiments, synthetic wastewater was used as an electrolyte and was made from tap water, 4.64 g/L Na_2HPO_4 , 1.75 g/L NaH_2PO_4 , 1.39 g/L NaHCO_3 and 0.165 g/L potassium nitrate (KNO_3) were added [32]. All chemicals used were laboratory grade and manufactured by Sigma-Aldrich, St. Louis, MO, United States.

2.4. Operating conditions in a two-chamber reactor (Article II)

Two MESRs were used for conducting the first experiment (Article II). One reactor was used as a control on open circuit potential (OCP), and the second as a MESR where the WE potential was controlled by potentiostat (Autolab PGSTAT30). A saturated calomel electrode (SCE) was used as a reference electrode (HACH radiometer analytical REF401) with a potential +244 mV vs standard hydrogen electrode (SHE). All of the WE potentials are referred to vs SHE throughout the thesis.

At the beginning of the experiment, the reactors were filled with synthetic wastewater, 4.22 L and 1.29 L in the WE and CE chambers, respectively. After that, the reactors were purged with N_2 until the dissolved oxygen (DO) concentration dropped below $0.30 \text{ mgO}_2/\text{L}$. The circulation pumps were then turned on and the WE potential was posed at $+394 \text{ mV}$ for 7 days to enhance inoculation. On the 8th day, the WE potential was changed to -306 mV to enhance denitrification.

The entire experiment lasted for 45 days, and during that time, gas from the WE chamber and water samples from the WE and CE chambers were collected every 2 to 4 days, depending on need. Each time samples were collected, the DO concentration, pH and temperature were measured and cyclic voltammetry (CV) measurements were performed.

When NO_3^- concentration in the WE chamber dropped below $5 \text{ mgN-NO}_3^-/\text{L}$, the KNO_3 was added. Sodium hydroxide (NaOH) and hydrogen chloride (HCl) were added to the WE and CE chambers accordingly to keep the pH at around 7.

2.5. Operating conditions in a single chamber reactor (Article III)

For the second experiment (Article III), three MESRs were used, all of which were operated differently. The experiment was conducted in many cycles, and the operating conditions of the cycles are described in Tables 1–3. Throughout the thesis, the cycles are referred as ‘cycle (1:2)’, where the first number indicates the reactor and the second number indicates the cycle related to the reactor. Whenever the reactor was assembled and filled with synthetic wastewater, the reactor was purged with N_2 until DO concentration dropped below $0.2 \text{ mgO}_2/\text{L}$. At the beginning of each cycle, the level of electrolyte was adjusted to the 5.5 L mark and the NO_3^- concentration was increased to $100 \text{ mgN-NO}_3^-/\text{L}$ by the addition of KNO_3 , unless stated otherwise. Every cycle was ended when the NO_3^- ions were depleted or no change in the concentration was registered. Since different REs were used, all the WE potentials are referred to vs SHE throughout the thesis.

Table 1. Reactor 1 and its operating information for every cycle. Potentiostat 1 (Autolab PGSTAT30 and software Nova 1.10, Metrohm Autolab B.V, Utrecht, The Netherlands). Potentiostat 3 (PARSTAT4000A and software VersaStudio 2.60.6, AMETEK Scientific Instruments, Berwyn, PA, USA). Saturated calomel electrode was used as a reference electrode (Radiometer Analytical REF401 Reference Electrode, Hach Company, Loveland, CO, USA) with a potential of +244 mV vs a standard hydrogen electrode

REACTOR 1				
Cycle	Period (days)	WE potential (mV vs SHE)	Initial NO₃⁻ concentration (mgN-NO₃⁻/L)	Potentiostat
1	0 to 215	various	15	1
<p>Objective: Searching for the WE potential where NO₃⁻ reduction occurs. Additional treatment:</p> <ul style="list-style-type: none"> • 200 mL of inoculum and 20 mL of trace element solution SL-4 were added. • After that, the reactor was connected with potentiostat and the WE potential was held at -320 mV on days 0–76. Later, it was changed multiple times: 77–81 (-356 mV); 82–84 (-406 mV); 85–87 (-456 mV); 88–90 (-506 mV); 91–97 (-556 mV); 98–101 (-606 mV); 102–109 (-656 mV); 110–122 (-706 mV); 123–140 (-156 mV); 141–146 (-56 mV); 147–150 (+43 mV); 152–215 (-756 mV). • On day 7, NO₃⁻ concentration was raised to 37 mgN-NO₃⁻/L. • On day 36, NO₃⁻ concentration was raised to 82 mgN-NO₃⁻/L. 				
2	216 to 259	-756	102	1
<p>Objective: Replicate the NO₃⁻ reduction.</p>				
3	260 to 302	-756	108	1
<p>Objective: Make sure that the electrolyte can be replaced and the NO₃⁻ reduction will still occur. Additionally, an analysis was conducted to assess microbial growth in the electrolyte. Additional treatment:</p> <ul style="list-style-type: none"> • Electrolyte was completely replaced with the new synthetic wastewater up to the 5.5 L mark and then 10 mL of trace element solution SL-4 was added. The electrodes were not replaced. • Then the reactor was purged with N₂ until DO concentration dropped to 0.20 mgO₂/L. • After that, the WE potential was kept at -756 mV. • During this cycle, additional samples were taken for microbial growth analysis. 				
4	302 to 350	-656	107	1
<p>Objective: Searching for the optimal WE potential for NO₃⁻ reduction.</p>				
5	351 to 399	-556	108	1
<p>Objective: Searching for the optimal WE potential for NO₃⁻ reduction.</p>				
6	400 to 456	-456	108	3
<p>Objective: Searching for the optimal WE potential for NO₃⁻ reduction.</p>				
7	459 to 574	-356	105	3
<p>Objective: Searching for the optimal WE potential for NO₃⁻ reduction.</p>				
8	575 to 612	-256	119	3
<p>Objective: Searching for the optimal WE potential for NO₃⁻ reduction.</p>				

Table 2. Reactor 2 and its operating information for every cycle. Potentiostat 2 (PMC-1000 and software VersaStudio 2.60.6, AMETEK Scientific Instruments, Berwyn, PA, USA). Ag/AgCl/saturated KCl was used as a reference electrode with a potential of +199 mV vs a standard hydrogen electrode

REACTOR 2				
Cycle	Period (days)	WE potential (mV vs SHE)	Initial NO ₃ ⁻ concentration (mgN-NO ₃ ⁻ /L)	Potentiostat
1	0 to 208	OCP	16	–
<p>Objective: OCP control with inoculum to make sure that the process cannot run without electricity.</p> <p>Additional treatment:</p> <ul style="list-style-type: none"> • 200 mL of inoculum and 20 mL of trace element solution SL-4 were added. • On day 7, NO₃⁻ concentration was raised to 34 mgN-NO₃⁻/L. • On day 36, NO₃⁻ concentration was raised to 71 mgN-NO₃⁻/L. 				
2	209 to 280	-756	202	2
<p>Objective: Abiotic control to make sure that at the WE potential of -756 mV, the NO₃⁻ ions are not reduced.</p> <p>Additional treatment:</p> <ul style="list-style-type: none"> • Reactor was opened and sterilized with ethanol. The electrodes were then replaced with a new set. • The reactor was then filled up to the 5.5 L mark with synthetic wastewater with an NO₃⁻ concentration of 202 mgN-NO₃⁻/L. After that, 20 mL of trace element solution SL-4 was added. • The reactor was then purged with N₂ until DO concentration dropped to 0.20 mgO₂/L. • After that, the reactor was connected with the potentiostat and the WE potential was set to -756 mV. 				
3	281 to 301	-656	110	2
<p>Objective: Searching for the optimal WE potential for NO₃⁻ reduction.</p> <p>Additional information:</p> <ul style="list-style-type: none"> • Since the reactor was contaminated and the bacteria grew to such an extent that we could see the NO₃⁻ ions being reduced on cycle 2 after ~20 days of abiotic test, we decided to run additional cycles to assess the NO₃⁻ reduction kinetics of the second reactor. • At the beginning of this cycle, the electrolyte level was not raised up to the 5.5 L mark. 				
4	302 to 336	-556	114	2
<p>Objective: Searching for the optimal WE potential for NO₃⁻ reduction.</p> <p>Additional treatment:</p> <ul style="list-style-type: none"> • At the beginning of this cycle, the electrolyte level was not raised up to the 5.5 L mark. 				
5	337 to 378	-456	123	2
<p>Objective: Searching for the optimal WE potential for NO₃⁻ reduction.</p>				

Table 3. Reactor 3 and its operating information. Potentiostat 2 (PMC-1000 and software VersaStudio 2.60.6, AMETEK Scientific Instruments, Berwyn, PA, USA). Ag/AgCl/saturated KCl was used as a reference electrode with a potential of +199 mV vs a standard hydrogen electrode

REACTOR 3				
Cycle	Period (days)	WE potential (mV vs SHE)	Initial NO₃⁻ concentration (mgN-NO₃⁻/L)	Potentiostat
1	0 to 30	-756	115	2
<p>Objective: Abiotic control to make sure that at the WE potential of -756 mV, the NO₃⁻ ions are not reduced.</p> <p>Additional treatment:</p> <ul style="list-style-type: none"> • To provide cleaner conditions, a completely new reactor was constructed. The reactor body and pump were sterilized with ethanol. • New set of electrodes was prepared and autoclaved with the sampling port gaps before the final assembly. • The synthetic wastewater and trace element solution SL-4 were also autoclaved. • Then the reactor was filled up to the 5.5 L mark with the solution and 20 mL of trace element solution SL-4 was added. • After that, the WE potential was held at -756 mV. 				

2.6. Chemical analysis (Articles I–III)

For all articles, the total carbon (TC), total inorganic carbon (TIC) and total organic carbon (TOC) were measured following the EVS-EN 1484 standard. TN was measured following the EVS-EN 12260 standard and a Vario TOC cube (Elementar Analysensysteme GmbH, Langensfeld, Germany) was used to conduct the measurements.

In Article I, the NH_4^+ , NO_3^- , NO_2^- , sulphate (SO_4^{2-}) and chlorine (Cl^-) concentrations were determined, using Ion chromatograph Metrohm 930 Compact IC Flex (Metrohm AG, Herisau, Switzerland), the column used was Metrosep A Supp5 100/4.0 (Metrohm AG, Herisau, Switzerland) with an effluent composition of 1.0 mM NaHCO_3 and 3.2 mM Na_2CO_3 . In Articles II and III, the NH_4^+ , NO_3^- , NO_2^- concentrations were measured spectrophotometrically using USEPA-8038 Hach Lange Nessler, SFS 5752 and SFS 3029 methods, respectively.

In Article I, a portable device YSI ProDSS (YSI Inc., Yellow Springs, OH, USA) was used to measure six parameters of the site, such as pH, turbidity (from spring 2018), temperature, DO, redox potential, and electrical conductivity (EC). SonTek FlowTracker (YSI Inc., Yellow Springs, OH, USA), a handheld acoustic Doppler velocimeter, was used to measure flow rate.

In Articles II and III, DO, pH and temperature were measured using the WTW Multi 3420 instrument (Xylem Analytics, Singapore) with WTW FDO 925, WTW pH-Electrode SenTix 940-3 and WTW FDO 925, respectively.

2.7. Gas analysis (Article II)

During the first MES experiment (Article II), the N_2O , methane (CH_4) and CO_2 gas fluxes were measured using the static closed-chamber method [33]. Gas samples were drawn from the 0.2–0.6 L and 0.1–0.5 L chamber headspace (WE chamber and CE chamber, respectively) in pre-evacuated (0.3 mbar) 50 mL glass bottles six times an hour (sample time-points: 0, 10, 20, 40, 50 and 60 minutes) using polypropylene syringes through a silicone tube.

The gas samples were analysed using a Shimadzu GC-2014 gas chromatograph combined with a Lofthfield automatic sample injection system, an electron capture detector for CO_2 and N_2O and a flame ionization detector for CH_4 [34]. Since the gas concentration in the chamber increased in a near-linear fashion, a linear regression was applied to calculate the gas fluxes. Flux measurements with a coefficient of determination (R^2) of 0.9 or greater were used in further analyses.

2.8. Quantitative Polymerase Chain Reaction (Article III)

During the second MES experiment (Article III), samples from three sets of electrodes were taken to analyse the presence and abundance of different genes. Each set consisted of 2 electrodes, WE and CE. The samples were crushed into a fine powder using a coffee bean grinder (Robert Bosch GmbH, Germany) in sterile conditions. The ground samples were weighed (0.25 g) and processed further for DNA (desoxyribonucleic acid) extraction. DNA was extracted using the Power-Soil DNA Isolation kit (MO BIO Laboratories Inc, Carlsbad, CA, USA) according to the manufacturer's recommendations. Homogenization was performed at 5000 rpm for 20 s (Precellys 24, Berlin Technologies, Montigny-le-Bretonneux, France). The extracted DNA samples were analysed for their concentrations and quality using a spectrophotometer Infinite M200 (Tecan AG, Grodig, Austria).

Qualitative polymerase chain reaction (qPCR) analysis was carried out to evaluate the abundances of the bacterial 16S rRNA gene, archaeal 16S rRNA gene and nitrogen transforming genes, such as bacterial ammonia monooxygenase (*amoA*), archaeal *amoA*, complete ammonia oxidation (comammox) *amoA*, nitrite reductase (*nirK*, *nirS*) and nitrous oxide reductase (*nosZI*) genes. The reaction was carried out in 10 μ L of the reaction mixture, consisting of 1 μ L of template DNA, 5 μ L of Maxima SYBR Green Master Mix (Thermo Fisher Scientific Inc, Waltham, MA, USA), optimized volumes of primers [35] and the remaining volume was nuclease-free water. All reactions were carried out in triplicate, with negative controls without template DNAs. The reactions were carried out using the RotorGene Q equipment (Qiagen, Valencia, CA, USA).

The gene-specific primer sets and the optimized reaction conditions were followed as described by Espenberg et al. [35]. The modifications were made for *nirS* and bacterial *amoA* primers: forward primer nirSCd3af was used instead of nirSC1F [36]; annealing temperatures for the qPCR program used were 55 $^{\circ}$ C and 57 $^{\circ}$ C for *nirS* gene and bacterial *amoA* gene, respectively. Comammox *amoA* genes were amplified using the comamoA AF and comamoA SR primers set [37]. The optimized program for comammox *amoA* gene was as follows: 10 min at 95 $^{\circ}$ C, 40 cycles of 15 s at 95 $^{\circ}$ C, 30 s at 55 $^{\circ}$ C and 30 s at 72 $^{\circ}$ C; the program ended with a melting curve analysis (temperature was increased from 65 $^{\circ}$ C to 95 $^{\circ}$ C at a rate of 0.35 $^{\circ}$ C/step and held at each step for 3 s).

The standard stocks used for determination of the gene abundances were prepared by serially diluting solutions of the target sequences (Eurofins MWG Operon, Ebersberg, Germany). The analysis of the runs was carried out using RotarGene[®] Series Software v.2.0.2 from Qiagen and LinRegPCR program v2020.0 [38]. Gene abundances were calculated as the mean fold differences between samples and corresponding 10-fold standard dilution in respective standards [38]. The gene abundances were represented as gene copy numbers per gram of dry weight (copies/g dw).

2.9. Calculation of the nitrate removal rate and the Faradaic efficiency (Article III)

The calculations of TN, removal rate of NO_3^- and NH_4^+ and Faradaic efficiency were performed during the second MESR experiment (Article III) as follows. The reactors were used as batch reactors, where each cycle can be divided into three phases (Figure 5): 1) lag phase, where the current density $|j|$ increases significantly and the NO_3^- removal rate accelerates; 2) stable phase, where the current density and NO_3^- removal rate stabilize to the constant value; and 3) end phase, which begins with a rapid current density $|j|$ drop and is associated with the depletion of NO_3^- . Since the cycles lasted over 20 days, it was impossible to determine the exact moment when NO_3^- was fully depleted. Therefore, to compare different cycles, the NO_3^- removal rates and Faradaic efficiency were calculated based on the data gathered during the stable phase (Figure 5).

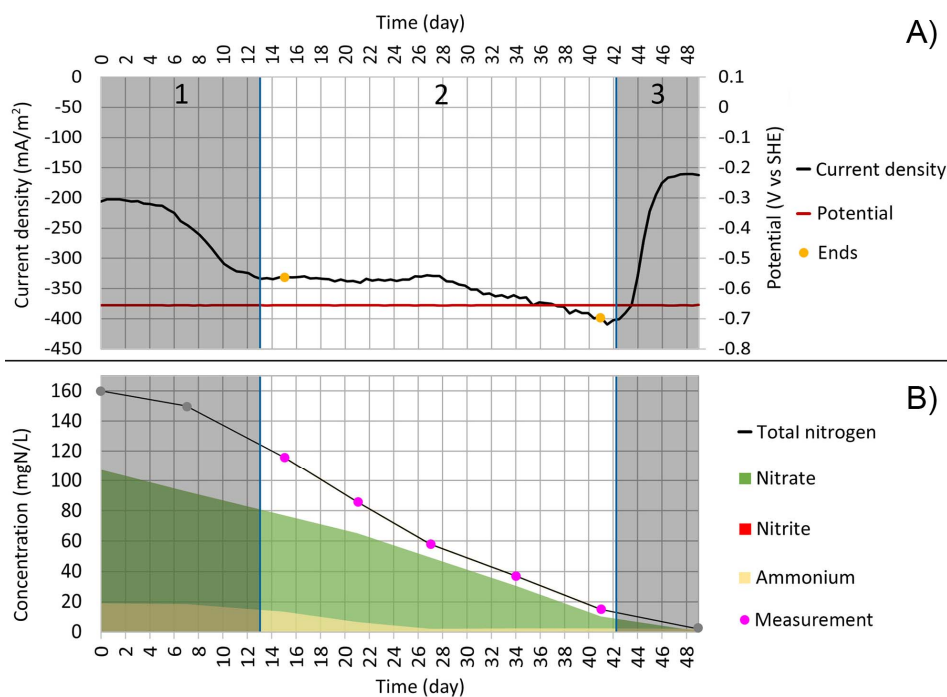


Figure 5. Closer view of the cycle (1:4) with phases 1 to 3. A) The yellow points represent start and end points of the period where the current density was integrated. B) The pink dots represent times when the water samples were taken during the stable phase. Grey dots show the times when the water samples were taken but were left out from the removal rate calculations. See Figure 11 for the explanation of other components on plots A and B

The rate of NO_3^- reduction was calculated by evaluating the quantity of reduced NO_3^- per day. For calculating the Faradaic efficiency, formula 3 was used.

$$\text{Faradaic efficiency} = \frac{\text{amount of } \text{NO}_3^- \text{ reduced in moles} \times 5}{\text{moles of electrons}} \times 100\% \quad (3)$$

Where moles of electrons are calculated based on the integrated charge, divided by the Faraday constant. Five indicates the number of electrons required to reduce one NO_3^- to N_2 according to the half reaction [39].

2.10. Statistical analysis (Articles I & II)

The analyses were performed using Statistica 10.0 (StatSoft Inc., Tulsa, OK, USA) and R software (version 3.4.4 and later a version 3.6.3, R Core Team, Vienna, Austria). The level of significance of $p < 0.05$ was accepted in all cases.

In the Article I, the Shapiro-Wilk tests were used to check the normality of variables. As the distribution of data deviated from normality, the nonparametric Mann-Whitney U test and Spearman's rank correlation were applied to compare the inlet and outlet of the system and both wetlands. Spearman's rank correlation was used to determine relationships between water parameters.

Similarly, to the first article, in the second article, the Shapiro-Wilk tests were used to check the normality of variables, but as the distribution of the data was skewed, the non-parametric Kruskal-Wallis's test was used to analyse the differences between water chemical parameters and GHG emissions between control and MESR. To evaluate different parameter effects on the current density, a Pearson r linear correlation was used.

2.11. Bibliometric analysis related to microbial fuel cell in constructed wetland (Article IV)

Many studies have shown that one possible way to enhance pollutant removal efficiency in CWs is the integration of MFC. Thus, a literature analysis related to CW-MFC was also conducted.

The Web of Science database was used to collect the data of literature about CW-MFC. The search was conducted for the period 2012–2020. After the data were gathered, the articles were filtered based on two criteria: 1) the experimental device meets the CW-MFC configuration requirements, specifically with the characteristics of the CWs of substrate, plant and other elements; and 2) the anode and cathode of the MFC must be embedded in the CW system. As a result, 135 out of 166 documents were used for further analysis. VOSviewer software (version 1.6.15, Leiden University, Netherlands) was used to generate network maps for key terms and keywords.

3. RESULTS AND DISCUSSION

3.1. Diffuse contamination of groundwater with nitrate and its mitigation to constructed wetlands in agricultural catchments (Article I)

Vända CW was constructed to treat the agricultural runoff water from nutrients and to evaluate the nutrient removal efficiency of a FWS CW. The average TN loading rate was 726 kg N/(ha × year). It turned out that the NO_3^- concentration in the water increased while passing through the CW from 4.1 to 5.4 mgN- NO_3^- /L. As a result, the NO_3^- removal efficiency was negative, at -31.6% (Figure 6.A). With NO_3^- , the TN concentration increased in the system by 27.7%, from 5.9 to 7.5 mgN/L (Figure 6.A). Seasonally the NO_3^- increase was also interesting, as during the summer, the concentration increased even more (45%). Overall, the results were surprising because in other studies the reported removal efficiencies have been much higher [9,40].

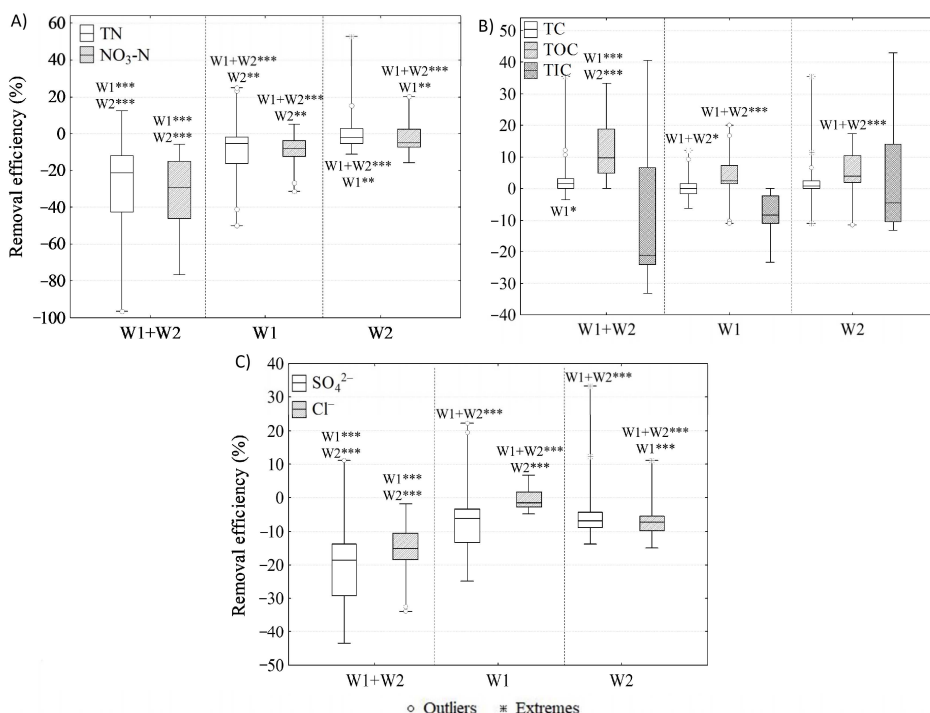


Figure 6. Removal efficiencies (%) of first wetland (W1), second wetland (W2) and both together (W1 + W2) during the study period for (A) total nitrogen (TN), nitrate (NO_3^- -N); (B) total carbon (TC), total organic carbon (TOC) and total inorganic carbon (TIC); (C) sulphate (SO_4^{2-}) and chlorine (Cl^-). Median, min/max, 25% and 75% quartile values are presented. Asterisks with numbers denote statistically significant differences between first wetland (W1), second wetland (W2) and both together (W1 + W2) according to the Mann-Whitney U test: *** $p < 0.001$, ** $p < 0.01$, * $p < 0.05$

The average TC concentration in Vända CW decreased from 68.2 to 66.3 mgC/L. TOC concentration in the system constituted around 75% of TC and its concentration decreased from 44.5 to 39.7 mgC/L. Therefore, the TC and TOC removal efficiencies were 2.9 and 12.4%, respectively (Figure 6.B). However, the TIC concentration in the CW increased from 30.3 to 31.0 mgC/L. With TIC, the SO_4^{2-} and Cl^- concentrations also increased in the CW (Figure 6.C), a kind of phenomenon usually related to groundwater seepage [41].

There was a strong positive correlation between TIC, SO_4^{2-} , Cl^- and NO_3^- , indicating that the additional NO_3^- entered the CW via groundwater. This was also the reason the NO_3^- removal efficiency was negative. On the other hand, the TOC: NO_3^- ratio was around 11:1, meaning that there was a deficiency of electron donors, which therefore hindered the denitrification and caused low NO_3^- removal efficiency[13].

3.2. Optimization of reactor design in experimental systems (Articles II & III)

To enhance NO_3^- removal efficiency in Vända FSW CW, implementation of a MESR was considered as a potential solution. At first, the two-chamber MESR was used to evaluate the possibility of conducting autotrophic denitrification in the MESR (Article II). The main reason for using a two-chamber MESR was the O_2 production on the CE, which could inhibit denitrification.

During the first experiment, the inoculation was conducted at a WE potential of +394 mV based on the paper by Pous et al [42]. The current density showed no change, although the NO_3^- concentration dropped below detectable range twice (Figure 7). At the same time, the NH_4^+ concentration increased; therefore, it is possible that the initial drop of NO_3^- could have been caused not only by denitrification, but also by dissimilatory nitrate reduction to ammonium or by Anammox [16,43]. However, similar trends were observed in both reactors, so the use of electrical manipulation did not seem to have a significant effect.

After the inoculation phase, the WE potential was changed to -306 mV on day 8. The current density $|j|$ started to increase, although the correlation was opposite to that which was anticipated (Figure 7). The current density should have been higher when more NO_3^- was present, as it has been presented in previous studies; however, in this case, it was the opposite[18,44]. The increase in current density $|j|$ was probably caused by the exposure of the WE to the gaseous phase because the water level decreased each time the water samples were taken. On the other hand, it shows that the electrical effect was negligible because later, in the second experiment (Chapter 3.2), where stable denitrification was achieved, the current density correlated with the depletion of NO_3^- as expected. During days 8 to 14, no significant discrepancies were observed between the MESR and the control reactor (Figure 7). The NH_4^+ concentration started to decrease and was most probably used in the Anammox process with NO_2^- [16]. After the NH_4^+ concentration dropped below 12 mgN- NH_4^+ /L, the NO_2^- concentration started to increase, indicating that the NO_2^- was produced in the system.

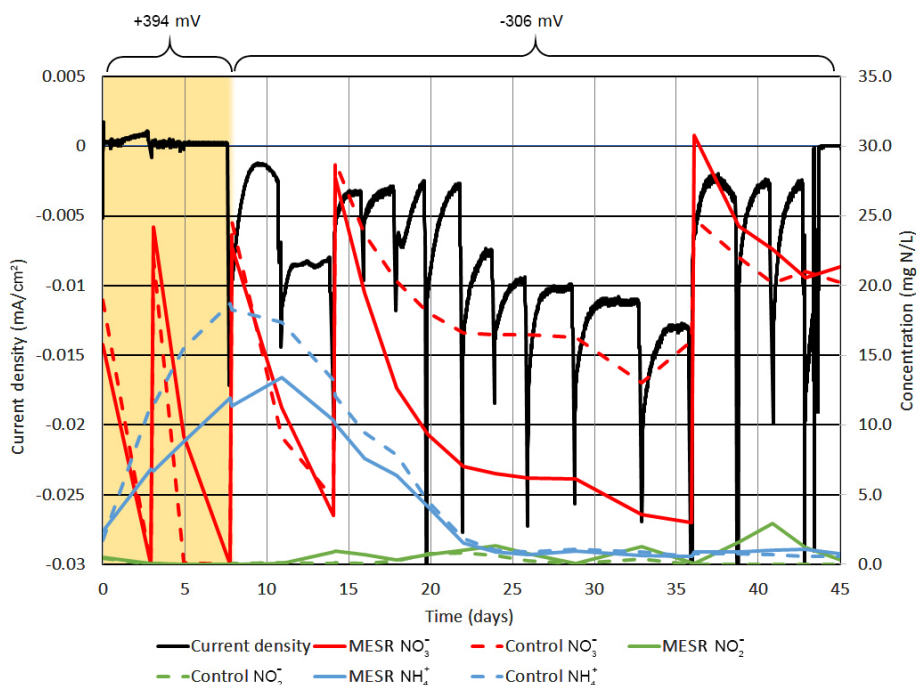


Figure 7. Current density, NO_3^- , NO_2^- and NH_4^+ concentration in WE chamber. The black line shows current density, the red lines NO_3^- , the green lines NO_2^- and the blue lines NH_4^+ concentration. Rapid increases in NO_3^- concentration on days 3, 7, 14 and 36 are related to the addition of KNO_3 . On days 0–7 (yellow background), the WE potential was posed at +394 mV. On day 8, it was switched to –306 mV

From day 14 to 36, the difference in the MESR and the control reactor appeared (Figure 7) and was most probably caused by the depletion of the easily degradable organic compounds introduced to the system with the inoculum. During that time, the NO_3^- removal rate decreased in both reactors, but in the MESR, the decrease was smaller. On day 36, the NO_3^- concentration was increased by adding KNO_3 . The NO_3^- removal rate remained higher until day 45, but then the experiment was ended because the CE was largely damaged by corrosion and the connection between the potentiostat and the CE was lost.

In the MESR, TN and NO_3^- removal efficiency was higher than in the control reactor. The average TN removal efficiency was 7.7 and 4.1%/day in the MESR and the control reactor, while the average NO_3^- removal efficiency was 8.5 and 3.7%/day, respectively (Figure 8). The discrepancy indicates that the WE might have been able to act as an electron donor after all. But compared to previous works, in which the NO_3^- removal rate ranged from 27 to 98 $\text{mgN-NO}_3^-/(\text{L} \times \text{day})$, the removal rate of 1.4 $\text{mgN-NO}_3^-/(\text{L} \times \text{day})$ registered in the MESR during the current experiment was very low[45,46].

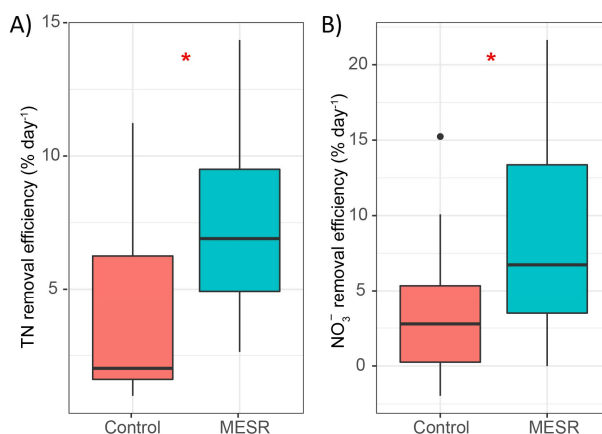


Figure 8. Nitrogen removal efficiency in microbial electrosynthesis reactor (MESR). **A)** Total nitrogen removal efficiency per day. **B)** NO₃⁻ removal efficiency per day. Median, min/max, 25% and 75% quartile values are presented. The asterisks denote statistically significant differences between the MESR and the control reactors * $p < 0.05$

pH was strongly influenced by electric manipulation. In the MESR, pH had to be constantly regulated to keep it in the optimal range by adding HCl and NaOH solution to the WE and CE chambers, respectively. The control reactor, however, did not need any pH regulation (Figure 9.A and B). pH is important as it influences bacteria and thereby NO₃⁻ removal efficiency [47].

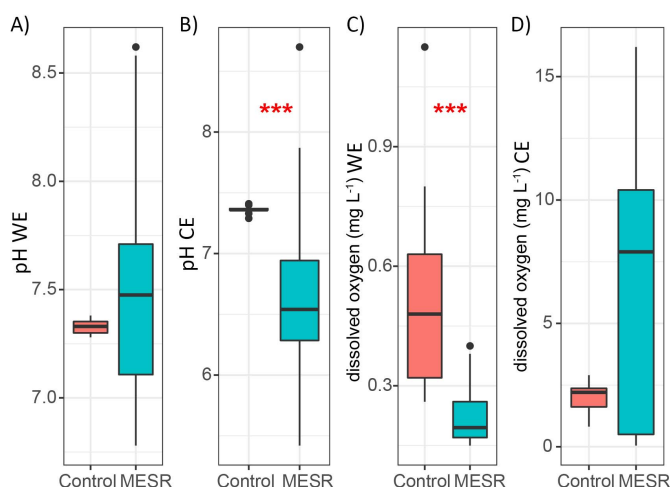


Figure 9. pH and dissolved O₂ concentration in MESR. **A)** pH in the working electrode (WE) chamber. **B)** pH in the counter electrode chamber (CE) chamber. **C)** Dissolved oxygen concentration in the WE chamber. **D)** Dissolved oxygen concentration in the CE chamber. Median, min/max, 25% and 75% quartile values are presented. The asterisks denote statistically significant differences between the MESR and control reactors * $p < 0.05$; *** $p < 0.001$

One aspect that might inhibit denitrification is high O_2 concentration, $0.5 \text{ mgO}_2/\text{L}$ and above [16]. Since the average DO concentration in a MESR WE chamber was around $0.23 \text{ mgO}_2/\text{L}$, it is unlikely that the O_2 could have been the cause for a low NO_3^- removal rate (Figure 9.C and D). However, in the MESR CE chamber, the DO concentration was much higher, with an average DO concentration of $6.7 \text{ mgO}_2/\text{L}$, meaning that the PEM can be successfully used as a barrier for O_2 .

Since the first approach did not show good enough results regarding NO_3^- removal and pH needed to be regulated continuously, a new attempt with a single-chamber MESR was performed (Article III). To suppress the O_2 production on CE (Figure 9.D), the electrodes were also swapped so that the GSA of the CE would be larger than the WE's surface area. In addition, graphite felt was used to make the electrodes. Titanium wire was used to make contacts so that it would not corrode like the previously used electrodes. To be sure that electroactive bacteria is present in the experiment, a pure culture of *Thiobacillus denitrificans* was used as an inoculum.

After the MESR (Reactor 1, Table 1) and control reactor (Reactor 2, Table 2) were assembled, the MESR WE's potential was held at -320 mV until day 76. In Reactor 2, the OCP was used. The NO_3^- concentration was increased twice, on days 7 and 36, since no changes were observed, with the expectation that the higher NO_3^- availability would help with inoculation (Figures 10 and 11).

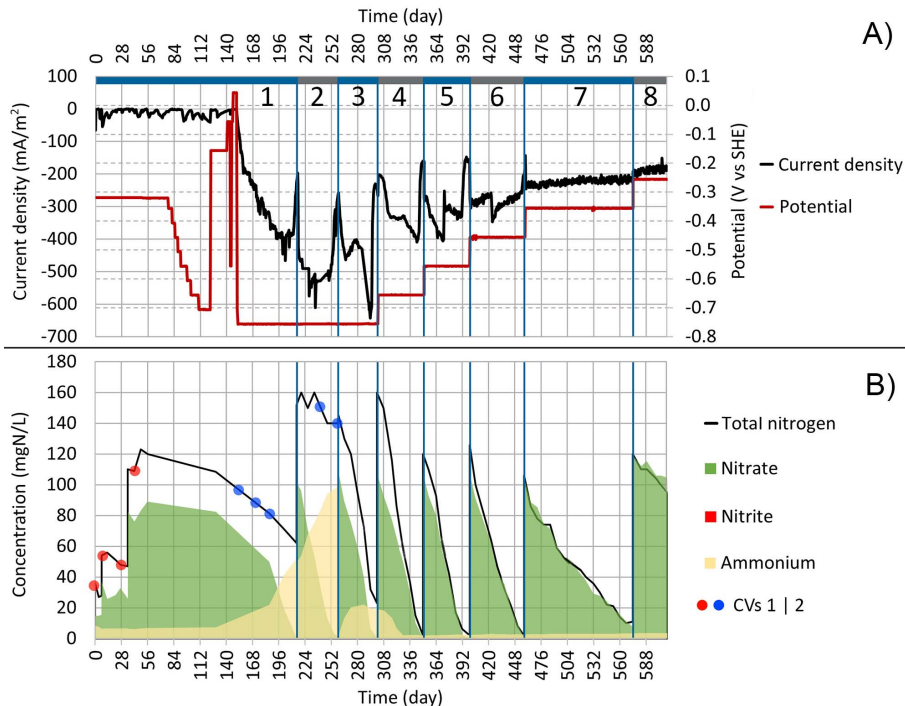


Figure 10. Dynamics of key parameters in Reactor 1 during the cycles (1:1) to (1:8). **A)** The change in current density and working electrode potential over time. **B)** Area graph of total nitrogen, nitrate, nitrite and ammonium concentrations in the electrolyte; the red and blue dots represent when the cyclic voltammetry measurements (shown in Figure 13) were performed. The blue vertical lines represent borders between the cycles

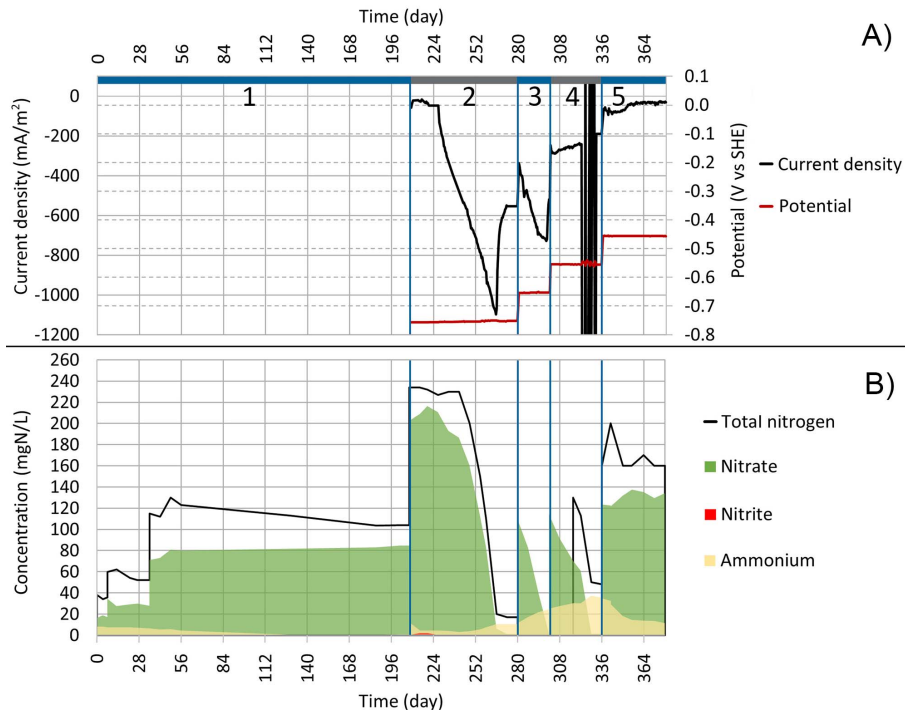


Figure 11. Dynamics of key parameters in Reactor 2 during cycles (2:1) to (2:5). See Figure 11 for explanation of plots A–B. During the cycle (2:1), the reactor was operated at open circuit potential

The DO concentration, measured on day 36, was 0.51 and 0.55 mgO₂/L for Reactors 1 and 2, respectively. Therefore, the O₂ was also in the optimal range for denitrification[48,49].

Since after 77 days, the NO₃⁻ concentration showed no change in Reactor 1 or 2, it was time to lower the WE potential until the NO₃⁻ reduction initiated. During days 77 to 122, the WE potential was lowered every 3 to 7 days by 50 mV (Figure 10). During that time, no water samples were taken to keep the disturbance level as low as possible. All monitoring was done using the change in current density. After the WE potential of -706 mV was used, the water samples, taken on day 122, showed no changes. On days 123 to 150, higher potentials -156, -56 and +43 mV were tried out without any success (Figure 10). Very low WE potentials were avoided at first because there was no knowledge about which potential $|E|$ would be too high and harm the microorganism's cell structure. The reduction peak at -300 mV (Figure 12) described in many MESR-related publications also appeared [30,50–53]. However, since no NO₃⁻ reduction was observed, the WE potential was lowered even more to -756 mV. On the next day (153), the current density $|j|$ started to increase (Figure 10). On the CV (Figure 12, inset section), the current density $|j|$, on lower WE potentials also started to increase (days 152–260).

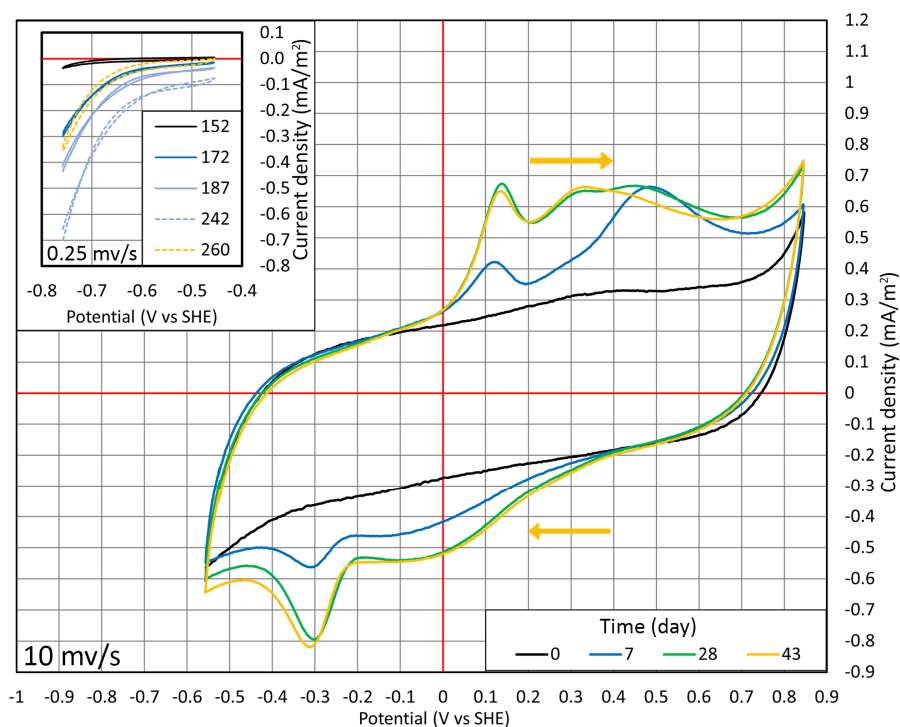


Figure 12. The cyclic voltammetry data during cycles (1:1) and (1:2). From days 0 to 43. Time points when the wide range measurements were conducted are shown as red dots in Figure 10.B. The inset section shows CV measurements on days 152 to 260 and the time points are shown in Figure 10.B as blue dots

On day 186, the water samples were taken and the NO_3^- concentration was decreased from 82 to 50 $\text{mgN-NO}_3^-/\text{L}$, meaning that NO_3^- reduction was finally achieved. By day 215, all the NO_3^- was reduced, but the adverse effect was that NH_4^+ concentration increased to 51.9 $\text{mgN-NH}_4^+/\text{L}$. In the control reactor (Reactor 2), the NO_3^- , NH_4^+ and TN concentrations remained the same as before (Figure 11), meaning that the NO_3^- reduction achieved in Reactor 1 was caused by the applied potential. In addition, the pH remained stable at 7.3 and 7.5 in Reactors 1 and 2, respectively.

After the first successful NO_3^- reduction in the MESR was achieved, two cycles (1:2) and (1:3) were conducted to replicate the results. During both cycles, the WE potential of -756 mV was used. For the cycle (1:2), NO_3^- concentration was increased by adding KNO_3 ; for the cycle (1:3), all the electrolyte was replaced. During both cycles, NO_3^- was reduced (Figure 10). pH remained stable in the range of 7.2 to 7.5; however, NH_4^+ was produced in both cycles. Usually, NO_2^- accumulates when denitrification is not conducted in optimal conditions, but it turns out that DNRA can also compete with denitrification in these systems [54–56].

As the NO_3^- reduction was achieved in Reactor 1 in cycles (1:1)–(1:3) and Reactor 2 showed no NO_3^- reduction in cycle (2:1), the abiotic control was conducted during cycle (2:2). For that, Reactor 2 was cleaned and sterilized with 99.8% ethanol and the electrodes were replaced (Table 2). After that, the WE was kept at a potential of -756 mV. For 19 days (days 208–227, on Figure 11), the current density $|j|$ stayed stable and no NO_3^- was reduced. After the 19th day, the current density $|j|$ started to increase and the NO_3^- reduction started. Since it took 19 days for the NO_3^- reduction to start, the possibility that the NO_3^- reduction in this system was purely electrochemical is low. This means that the reactor became contaminated at some point, probably while water samples were taken. Gene analysis showed that genes related to denitrification were present. To prove that the NO_3^- reduction would not initiate without inoculum, a second abiotic control was conducted (Table 3). For that, a completely new reactor was built and sterilized. During that cycle (3:1), which lasted for 30 days, no NO_3^- was reduced (Figure 13), although the current density $|j|$ increased. Therefore, the MESR can be used for reducing NO_3^- in situations where it would not be reduced otherwise. It works only if there is cooperation between microorganisms and electricity.

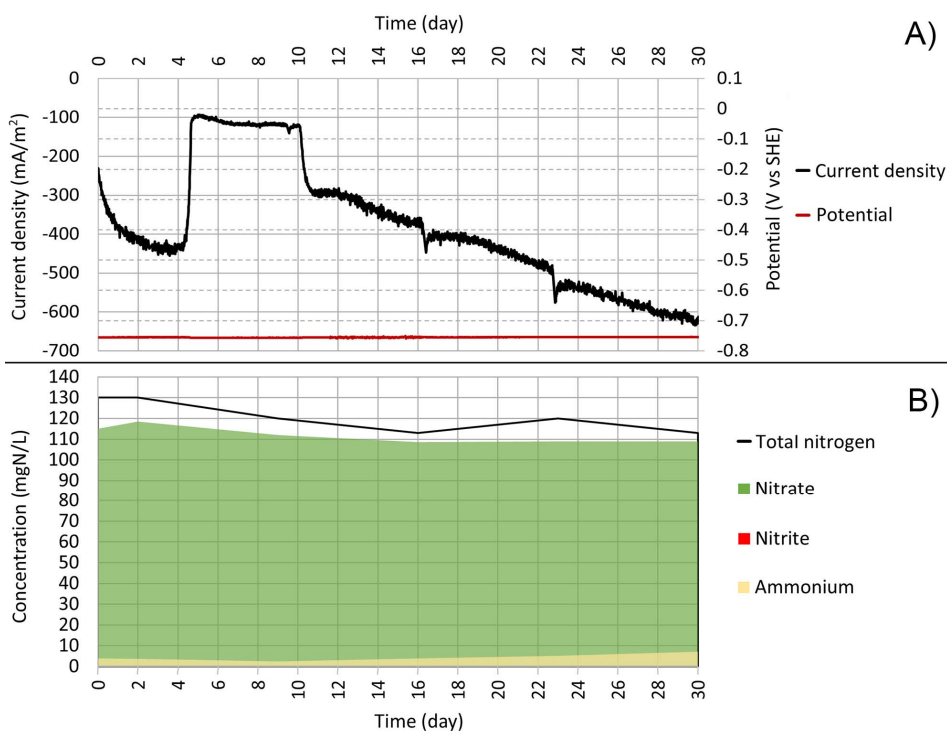


Figure 13. Dynamics of key parameters in Reactor 3 during the second abiotic control. See Figure 10 for explanation of plots A–B

3.3. Optimization of operating conditions in experimental systems (Article III)

To understand how the WE potential influences the processes in the MESR, various WE potentials were used during the second MES experiment (Article III). Also, the Faradaic efficiency and NO_3^- removal rate were calculated to see which WE potential is optimal for removing NO_3^- from water.

At a WE potential of -756 mV, NO_3^- reduction occurred, but the reduction was so intense that NH_4^+ was produced. Since it was unclear how much the WE potential could be increased, higher WE potentials were tested during cycles (1:4)–(1:8). It was found that after the NO_3^- reduction was initiated, the WE potentials can be decreased and the NO_3^- reduction would not stop. At least at the potential of -256 mV, reduction of NO_3^- was still observed (Figures 11.B and 14.A). Since the NO_3^- started to reduce in Reactor 2, parallel measurements were conducted during the cycles (2:3)–(2:5). NO_2^- concentration increased above the detection limit for a short period of time in Reactor 2 at the beginning of cycle (2:2) (Figure 11), but no accumulation of NO_2^- was observed during the experiment. NH_4^+ was produced at WE potentials of -756 mV and -656 mV; however, at higher WE potentials, NH_4^+ production ceased (Figure 14.A). At WE potentials -656 mV and above, the amount of NH_4^+ that has previously accumulated decreased. This means that in the right conditions, the MESR could even be used to remove NH_4^+ from water (Figure 10).

TN and NO_3^- removal rates were highest at the WE potential of -656 mV and the removal rates were 3.9 and 3.8 ± 1.2 mgN/(L \times day), respectively (Figure 14.A). At the WE potential of -256 mV, the NO_3^- was still being reduced, but the speed of reduction decreased significantly. As expected, the current density $|j|$ also decreased by increasing the WE potential (Figure 14.B). This happens because the WE potential gets closer to the OCP and therefore the rate of redox processes decreases. Highest Faradaic efficiency 71% was achieved at the WE potential of -656 mV (Figure 14.B).

In conclusion, even small changes in WE potential can influence the ongoing processes and the Faradaic efficiency by a substantial amount. Therefore, it is very important to choose the right potential, after the NO_3^- reduction is initiated, in order to find the balance between dominating processes, removal rate and Faradaic efficiency.

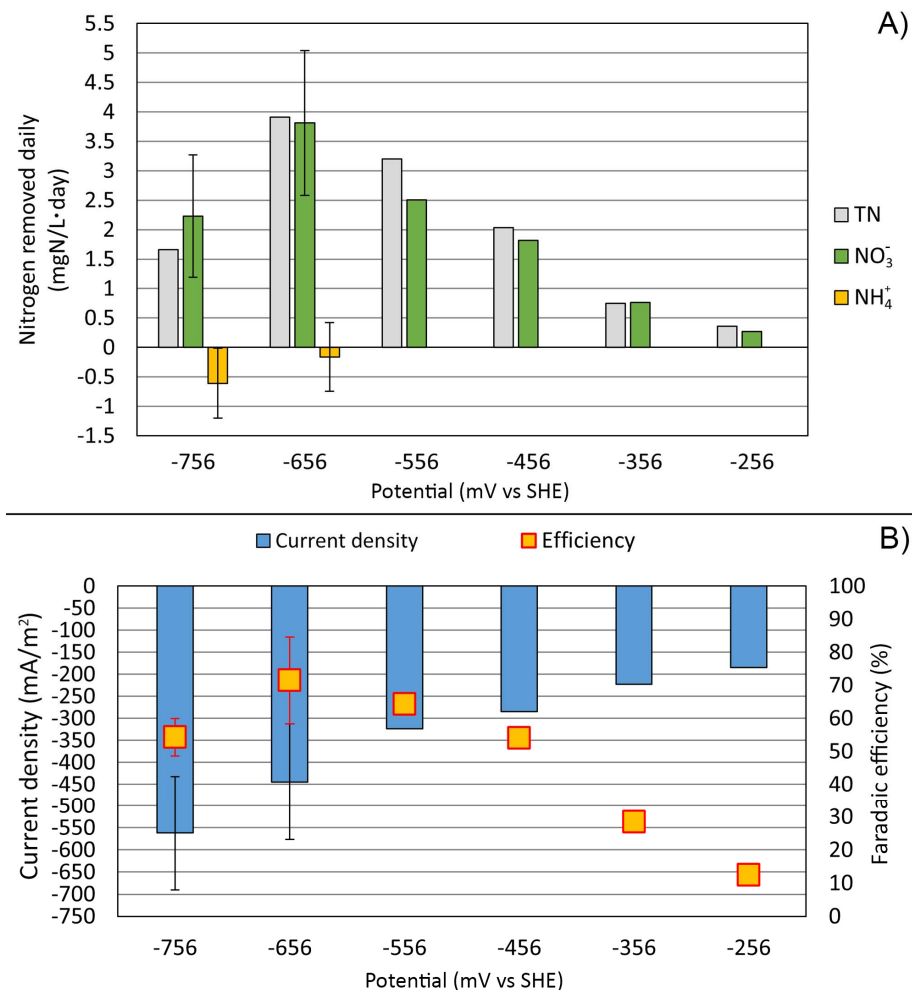


Figure 14. Relationship between electrode potential (mV vs standard hydrogen electrode (SHE)), nitrogen removal rate and current density. **A)** The daily removal rate for total nitrogen (TN), nitrate (NO₃⁻) and ammonia (NH₄⁺) at different working electrode (WE) potentials. **B)** The Faradaic efficiency and the average current density are shown for different WE potentials. At the WE potential -756 mV there are 3 replicate measurements and at -656 mV there are 2 replicate measurements for NO₃⁻ and NH₄⁺. Error bars represent standard deviations

3.4. Changes in nitrogen-related functional genes in microbial electrosynthesis reactor (Article III)

To understand how electrical manipulation influences the microbial community, the abundance of bacterial and archaeal 16S rRNA, bacterial and comammox *amoA*, *nirS*, *nirK* and *nosZI* genes were quantified. Three electrode sets were collected for gene analysis. Electrode set 1 was used for 612 days in Reactor 1 for all 8 cycles (1:1) to (1:8) (Figure 10). Electrode set 2 was used for 169 days in Reactor 2 cycles (2:2) to (2:5) (Figure 11) and electrode set 3 was used for 30 days in Reactor 3 cycle (3:1) (Figure 13).

Bacterial 16S rRNA and archaeal 16S rRNA genes followed the trend where the electrode that was in use for longer time had a higher gene abundance (Figure 15). Electrode set 1 had highest gene abundances on the WE, except *amoA* gene, which was most prominent on electrode set 2. This might have been because this electrode set was collected while NH_4^+ was still present in the reactor (Figure 11). For electrode set 1, the reactor had been working for a long time without NH_4^+ before it was collected and therefore the *amoA* gene abundance might have decreased. Interestingly, electrode set 3, which was collected from Reactor 3, where abiotic control was conducted, also showed a high abundance of nitrogen-cycle-related genes (Figure 15).

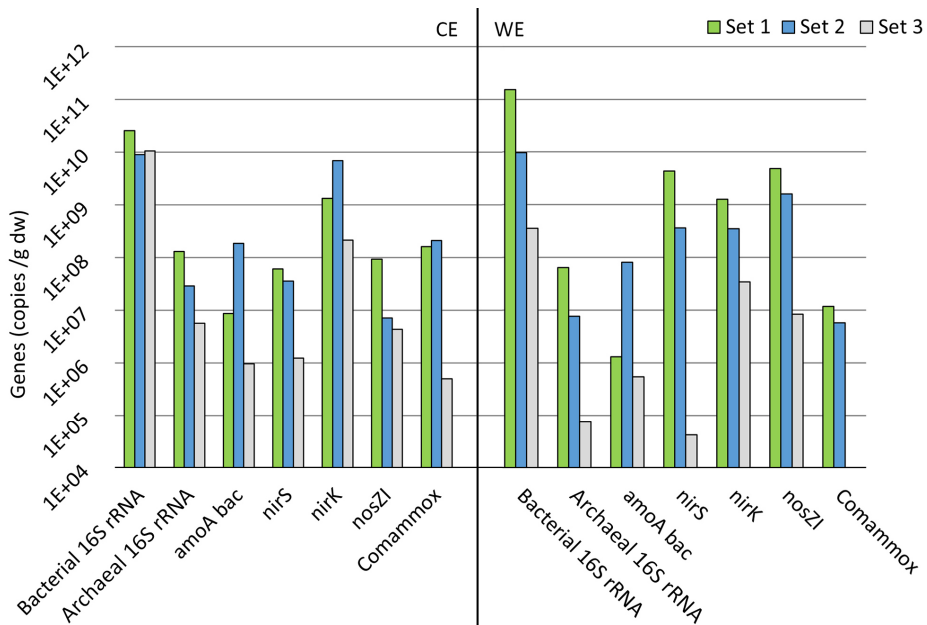


Figure 15. Gene abundances of electrode sets 1 to 3 on a logarithmic scale. Counter electrode data is shown in CE and working electrode data in WE section. See chapter 3.4 for the explanation of gene symbols and electrode names.

However, NO_3^- reduction was not observed during the test (Figure 13). The *nirS* gene related to denitrification's second step, where NO_2^- is reduced to nitric oxide, showed significantly lower abundance, which might be the reason NO_3^- reduction did not occur in Reactor 3.

Over three electrode sets, the average *nirS* and *nosZ-I* gene abundance was significantly higher on WEs (Figure 16). Those previously mentioned genes are more abundantly found in denitrifiers; therefore, there is relevant evidence of complete denitrifiers being present on the WE [57]. Abundance of *amoA* and comammox genes was higher on the CE (Figure 16). Those genes are related to oxidizing ammonia and it was therefore a predictable finding [10]. This is because during the oxidation of ammonia, there is a need for electron acceptors, and the CE in the current reactors could be used for that purpose. The presence of ammonia-oxidizing bacteria may also be a reason the NH_4^+ was removed from the system during the cycle (1:4) (Figure 10).

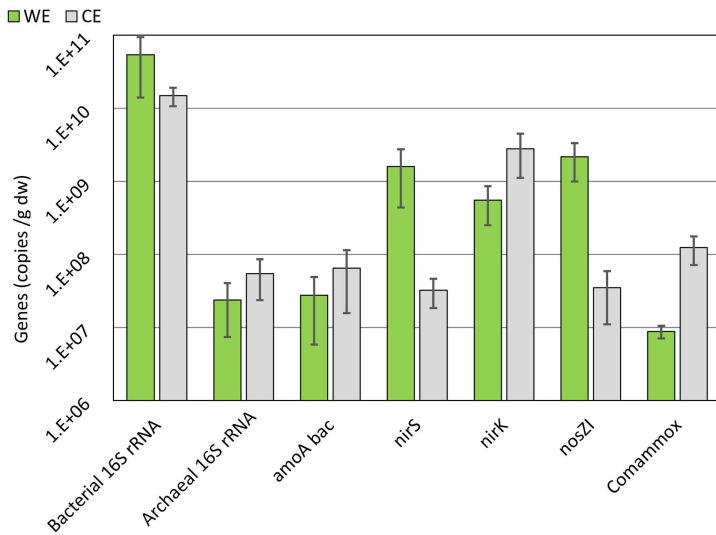


Figure 16. Average abundances of gene copies on working electrode (WE) and counter electrode (CE) over all three electrode sets on a logarithmic scale. 16S rRNA, *nirK*, bacterial *amoA*, *nirS*, *nosZ-I* and comammox gene abundances are shown. See chapter 3.4 for the explanation of gene symbols. Error bars are used to show standard error

3.5. Greenhouse gas fluxes in microbial electrosynthesis reactor (Article II)

From an environmental sustainability point of view, N_2O emissions should be estimated and considered in MESR designs [58]. Although NO_3^- removal efficiency was higher in the MESR, the N_2O emission in the MESR $-0.64 \text{ mgN}/(\text{m}^2 \times \text{h})$ was significantly lower compared to the control reactor's $0.01 \text{ mgN}/$

($\text{m}^2 \times \text{h}$) (Figure 17.A). Emission of CO_2 was also lower in the MESR $-5.32 \text{ mgC}/(\text{m}^2 \times \text{h})$, while in the control the emission was $43.79 \text{ mgC}/(\text{m}^2 \times \text{h})$ (Figure 17.B). The MESR was acting as a sink for CH_4 , with the average fluxes of -0.31 and $-0.08 \text{ mgC}/(\text{m}^2 \times \text{h})$ for the MESR and the control, respectively (Figure 17.C).

Lower CO_2 and N_2O emissions in the MESR are expected because in the MESR, the WE acts as an electrode donor and the possibility for complete denitrification to occur is much greater [13]. Because of the autotrophic denitrification where CO_2 is used as carbon source by microorganisms, lower CO_2 emission were also expected (reaction 1). Lower CH_4 emission in the MESR might have been caused by methane-dependent nitrate reduction to ammonium because, at the same time, NH_4^+ concentration in the MESR increased [43].

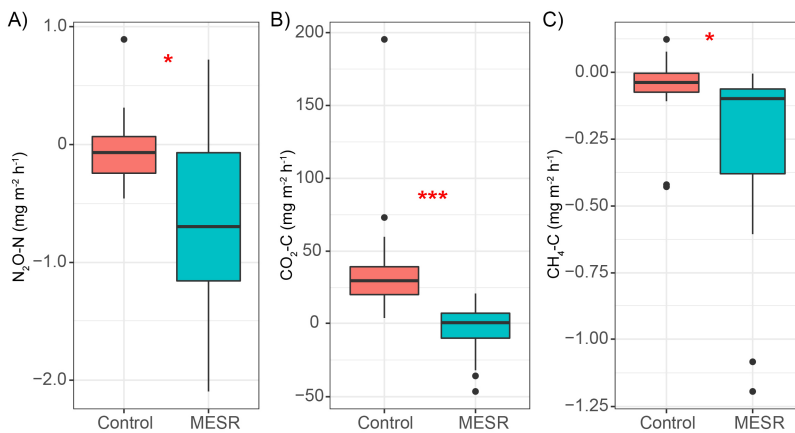


Figure 17. Gas fluxes in the MESR and control reactors. **A)** N_2O , **B)** CO_2 and **C)** CH_4 . Median, min/max, 25% and 75% quartile values are presented. The asterisks denote statistically significant differences between the MESR and control reactors * $p < 0.05$; *** $p > 0.001$

3.6. Bibliometric analysis related to microbial fuel cell in constructed wetland (Article IV)

The need to advance the treatment processes in CWs has significantly increased the number of studies related to CW-MFC. Since 2012, published studies have increased from 1 to 28 in 2019 (Figure 18), resulting in at least 135 studies being published in that time frame. The articles gathered were divided into four categories based on their focus: 1) contaminant removal and bioenergy generation; 2) energy application; 3) microbiology; and 4) structure optimization. In 2012 and 2013, the focus was on contaminant removal efficiency and energy production. In 2013, Zhao et al. (2013) were able to reduce the chemical oxygen demand (COD) by 76.5% in swine wastewater while achieving a power density

of 9.4 mW/m² [59]. In 2014, the first publications investigating how different electrode materials, hydraulic regimes or cell structures could help optimize the CW-MFC appeared [60–62]. Since 2015, the articles have started to investigate the topic in greater detail. The effects of different plants, substrates and microbes on power generation and purification efficiency have been evaluated in CW-MFCs [63–67].

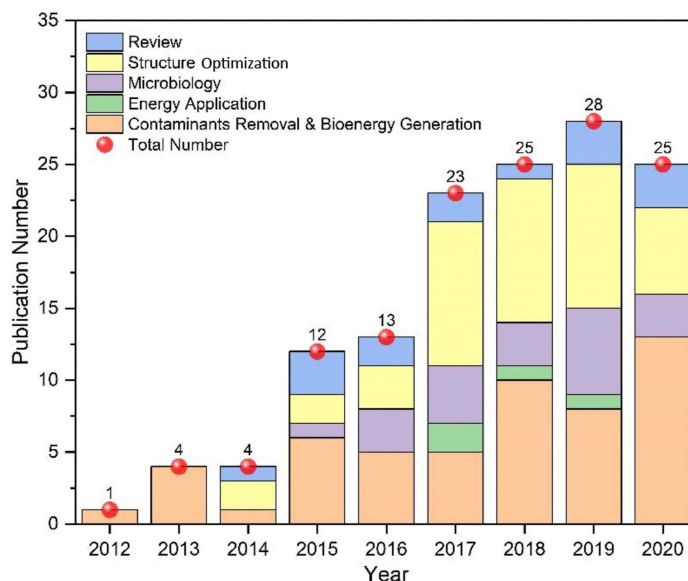


Figure 18. The number of publications per year and research categories in CW-MFC

By analysing the key terms, it is possible to apprehend the main aspects being researched. The red cluster, where the central term is coulomb efficiency, mainly comprises studies related to bioelectricity performance (Figure 19). It was found that closely related terms included ‘bioelectricity’, ‘electrode spaces’, ‘energy recovery’ as well as ‘oxygen’ and ‘COD removal rate’. The green cluster is more related to studies where microbiology is an aggregative term. The most frequent term in this cluster is ‘relative abundance’, followed by ‘macrophyte’, ‘microbial community’, ‘geobacter’ and ‘microcosm’. The blue cluster is formed by terms related to different pollutants, such as ‘azo dye’, ‘sulfamethoxazole’ and other problematic aspects like ‘antibiotic resistance genes’. In the yellow cluster, the focus is more on the removal performance of traditional contaminants like ‘total phosphorous’, ‘total nitrogen’, ‘nitrogen removal’ and ‘denitrification’.

Overall, the research topics related to CW-MFC have become more technical with time and the approach is no longer so broad. The focus is on increasing contaminant removal efficiency and power output as well as on evaluating the ability to remove different problematic pollutants like azo dye.

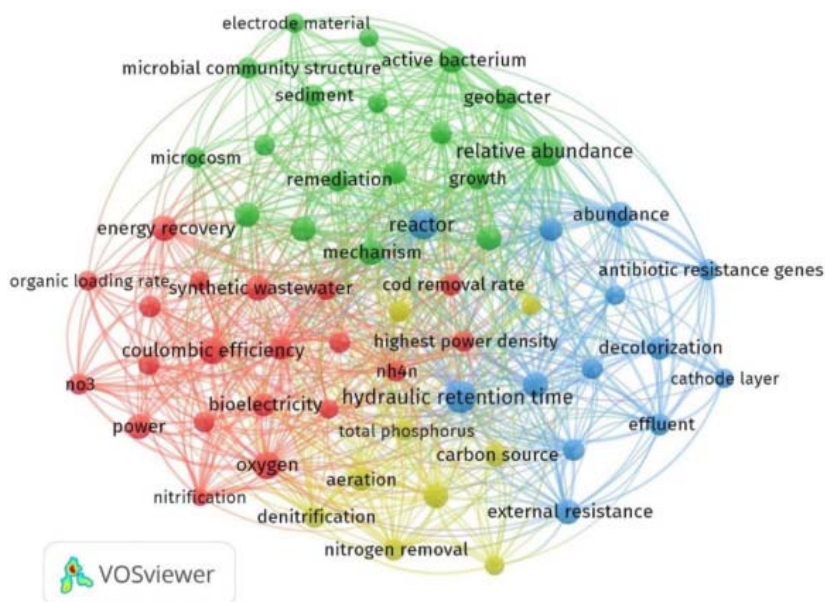


Figure 19. Key term occurrence network visualization map in CW-MFC. (A) Red cluster most related to bioelectricity generation performance; (B) Green cluster focuses on microbiology-related studies; (C) Blue cluster is related to the removal of problematic pollutants; (D) Yellow cluster focuses on removal performance of traditional contaminants

MFC-CW is a good solution when enhancing pollutant removal efficiency is the goal. However, it should be emphasized that unlike CW, which has been widely applied with a large number of field-scale applications worldwide, the current CW-MFC systems are in the pilot-scale or lab-scale stage. A lot of research has been conducted in relation to CW-MFCs but no article was found where NO_3^- could be removed in an absence of electron donors.

3.7. Synthesis of 3.1–3.6

The biggest problem with treatment efficiency in the Vända in-stream CW was related to nitrogen removal efficiency. Concentration of nitrogen compounds TN, NO_3^- , NO_2^- increased in the wetland by 27.7%, 31.6% and 15.1%, respectively (Figure 6). The study showed that the nutrient removal efficiency of the CW was seriously affected by groundwater. On the other hand, CWs can still reduce some of the pollution originating in groundwater, therefore making these systems more multifunctional.

The nitrogen of Vända CW is mainly in the form of NO_3^- and the average TOC to NO_3^- ratio was 11:1, which can be considered low. Low NO_3^- removal efficiency is usually related to the lack of electron donors and this might be the case in the current CW. Therefore, implementing a MESR could be a good solution to

overcome that obstacle. In a small-scale reactor, a stable NO_3^- reduction by autotrophic denitrification in the constructed MESR was achieved. The optimal potential was found to be -656 mV, where the highest Faradaic efficiency of 71% and NO_3^- removal rate of 3.8 ± 1.2 mgN- $\text{NO}_3^-/(\text{L} \times \text{day})$ were registered (Figure 14).

Based on the NO_3^- removal rate achieved during the second MES experiment (Article III), the WE's GSA should be *ca* 964 m^2 in order to completely remove NO_3^- from the water in Vända CW (Equations 4–8).

MESR NO_3^- removal rate per day =
MESR removal rate per litre per day \times MESR volume

$$\frac{3.8 \text{ mgN-NO}_3^-}{\text{L} \times \text{day}} \times 5.5 \text{ L} = \frac{20.9 \text{ mgN-NO}_3^-}{\text{day}} \quad (4)$$

MESR NO_3^- removal rate per m^2 per day =
MESR NO_3^- removal rate per day / working electrode's GSA

$$\frac{20.9 \text{ mgN-NO}_3^-}{\text{day}} \times \frac{1}{225 \text{ cm}^2} \times \frac{10\,000 \text{ cm}^2}{1 \text{ m}^2} = \frac{929 \text{ mgN-NO}_3^-}{\text{m}^2 \times \text{day}} \quad (5)$$

Average total nitrogen load in CW per year =
Average total nitrogen load in CW per ha per year \times CW surface area

$$\frac{726 \text{ kgN}}{\text{ha} \times \text{year}} \times 0.45 \text{ ha} = \frac{327 \text{ kgN}}{\text{year}} \quad (6)$$

Average total nitrogen load in CW per day =
Average total nitrogen load in CW per year / days in a year

$$\frac{327 \text{ kgN}}{\text{year}} \times \frac{1 \text{ year}}{365 \text{ days}} = \frac{0.896 \text{ kgN}}{\text{day}} \quad (7)$$

WE's GSA =
Average total nitrogen load in CW per day / MESR NO_3^- removal rate
per m^2 per day

$$\frac{896 \text{ gN}}{\text{day}} \div \frac{0.929 \text{ gN-NO}_3^-}{\text{m}^2 \times \text{day}} = 964 \text{ m}^2 \quad (8)$$

As in Vända CW there is a groundwater seepage and in the 2nd wetland the groundwater intrusion is monitored, the best position for implementing the MESR would be near the exit (Figure 2). By calculating the volume of the electrodes necessary to enhance denitrification, it is possible to evaluate whether the last section in Vända CW is large enough to accommodate the MESR. The volume of the last section is *ca* 80 m^3 (Equation 9).

Volume of the last section in CW = width × length × depth

$$10 \text{ m} \times 20 \text{ m} \times 0.4 \text{ m} = 80 \text{ m}^3 \quad (9)$$

The optimal electrode configuration should be assessed before, but one possible configuration would be the one where WEs are placed between the CEs. During the second experiment, the CE's GSA was 3.65 times larger than WE's GSA. The graphite felt used to construct the electrodes was 3 mm thick. The total volume of the electrodes is calculated in formula 10 and based on the calculations (Equations 9 and 10), it can be said that the MESR could fit in Vända CW.

Total volume of electrodes =
(ratio of CE:WE GSA in MESR + 1) × calculated WE GSA × electrode's
material thickness

$$(3.65 + 1) \times 964 \text{ m}^2 \times 0.003 \text{ m} = 13.4 \text{ m}^3 \quad (10)$$

Based on the current density data obtained during the second MES experiment (Article III), the current source must have a current output of at least 434 A (Equation 11). And it would be wise to split the MESR into sections to ensure equal WE potential distribution. This way, there is a possibility to use multiple power sources, with lower current outputs and increase the controllability of the reactor.

Minimal current output = current density × WE's GSA

$$\frac{0.45 \text{ A}}{\text{m}^2} \times 964 \text{ m}^2 = 434 \text{ A} \quad (11)$$

Taking energy consumption into consideration, the MFC is preferred since it is possible to produce electricity with MFC. But in a situation where the treatable water lacks electron donors, the MFC could not be used. This is the case because in the MFC, the reactions must occur spontaneously. In the absence of electron donors, denitrification would not occur and NO_3^- would not be removed, meaning that the MFC would not work. Because of that, the MESR could be a good solution for enhancing nitrogen removal efficiency in Vända FWS CW.

One possible way to produce the electricity for the MESR is using solar cells. Based on the current needed, it is possible to make assumptions about how powerful the solar cell system would have to be. During the experiment, only the potential of the WE was measured, as a result of which there is no knowledge about the potential difference between WE and CE. But it should be in the range of 1–2 V. For the following calculations, the more conservative potential was used. By multiplying the potential by the current, it is possible to calculate the power of the system. By adding the time factor, it is possible to say how much power is used in a year (Equations 12–13).

Power = potential \times current

$$2 V \times 434 A = 868 W \quad (12)$$

Power consumption in kWh per year = power $\times \frac{\text{hours}}{\text{day}} \times \frac{\text{day}}{\text{year}}$

$$868 W = 0.865 kW \quad (13)$$

$$0.865 kW \times \frac{24 \text{ hours}}{\text{day}} \times \frac{365 \text{ days}}{\text{year}} = 7577 \text{ kWh}$$

Yearly power consumption (Equation 13) is mainly used to dimension the solar cell systems. For calculating the power of the solar cell system, a solar cell calculator was used [68]. It takes the weather data and geographical position into consideration when calculating the power. Based on the total yearly power production, the power of the solar cell system would have to be 8 kW, meaning that it would be necessary to use 32 solar cells with a surface area of 53 m² to produce enough electricity. However, it must be taken into the consideration that during the winter, there would be a deficit in electricity production and during the summertime, a surplus in electricity production.

Based on current results, the MESR could increase NO₃⁻ removal efficiency in Vända CW, but a pilot-scale study should be conducted before experimenting with large scale systems. It is necessary to evaluate different electrode configurations and find the optimal GSA ratio of CE and WE. Since the CW is a continuous flow system, an experiment should be conducted to assess how the flow rate influences NO₃⁻ removal efficiency. If the flow rate is too high in the last section, it could be made deeper. The autotrophic denitrification removal efficiency in the MESR should be evaluated at lower temperatures because, at a lower temperature, the denitrification rate is usually lower. In Vända CW, the water temperature was much lower compared to the one used in the MESR experiments. MES technology in itself is proven to work and is therefore a very promising solution for enhancing reaction rate driven by microorganisms.

4. CONCLUSIONS

The Vända in-stream CW showed a strong seasonal dynamic over the study period, depending on nutrient runoff from the surrounding fields, fertilization and groundwater seepage and rainfall/snowmelt events. Concentration of nitrogen compounds TN, NO_3^- , NO_2^- increased on average in the wetland by 27.7%, 31.6% and 15.1%, respectively, and the increases were even higher during summer.

Various tests were conducted to achieve NO_3^- reduction in the MESR via denitrification. The optimal potential was found to be -656 mv vs SHE, where the highest Faradaic efficiency of 71% and NO_3^- removal rate of 3.8 ± 1.2 mgN- NO_3^- / (L \times day) were registered. The MESR also showed lower GHG emissions. The N_2O fluxes showed a much larger variation in the MESR, but the mean value was significantly lower than in the control reactor: -0.64 and -0.01 mgN/($\text{m}^2 \times \text{h}$), respectively. This means that the use of a MESR in a CW can have a positive effect regarding GHG emissions.

Microbiological analysis supported denitrification as the main process of nitrate removal in the MESR studied. The average *nirS* and *nosZ-I* gene abundance on all three electrode sets was significantly higher on WEs than CE. This likely indicates complete denitrification on the WE. Ammonia-oxidizing bacteria characterized by *amoA* and *comammox* genes showed higher abundance on the CE. During the oxidation of ammonia, there is a need for electron acceptors; the CE in the current reactors could be used for this purpose. A high abundance of ammonia-oxidizing bacteria could also be the reason the NH_4^+ was removed from the system during the cycle (1:4).

A literature analysis was conducted during the experiments to see whether CW-MFC could be used for enhancing NO_3^- removal efficiency. Many topics researched that are related to CW-MFC are similar to topics related to MES. However, no studies were found, where MFC have been used to reduce NO_3^- in a situation where the electron donor concentration is low. Therefore, the MESR seems to be the technology to work towards now.

Based on the results achieved during the experiments with the MESR, it can be said that the MES is a promising technology to enforce denitrification in situations where the electron donor concentration is low. The Vända in-stream CW is a potential candidate where the MESR could be applied, but some pilot-scale studies are necessary before going large scale.

REFERENCES

1. *Guidelines for Drinking-Water Quality: Fourth Edition Incorporating the First Addendum. Licence: CC BY-NC-SA 3.0 IGO*; Geneva, 2017;
2. Pärn, J.; Henine, H.; Kasak, K.; Kauer, K.; Sohar, K.; Tournebize, J.; Uemaa, E.; Välik, K.; Mander, Ü. Nitrogen and Phosphorus Discharge from Small Agricultural Catchments Predicted from Land Use and Hydroclimate. *Land Use Policy* **2018**, *75*, 260–268, doi:10.1016/J.LANDUSEPOL.2018.03.048.
3. Camargo, J.A.; Alonso, Á. Ecological and Toxicological Effects of Inorganic Nitrogen Pollution in Aquatic Ecosystems: A Global Assessment. **2006**, doi:10.1016/j.envint.2006.05.002.
4. Flem, B.; Reimann, C.; Birke, M.; Banks, D.; Filzmoser, P.; Frengstad, B. Inorganic Chemical Quality of European Tap-Water: 2. Geographical Distribution. *Applied Geochemistry* **2015**, *59*, 211–224, doi:10.1016/J.APGEOCHEM.2015.01.016.
5. el Khattabi, J.; Louche, B.; Darwishe, H.; Chaaban, F.; Carlier, E. Impact of Fertilizer Application and Agricultural Crops on the Quality of Groundwater in the Alluvial Aquifer, Northern France. *Water, Air, & Soil Pollution* **2018**, *229*, 1–15, doi:10.1007/S11270-018-3767-4.
6. Barroso, M.F.; Ramalhosa, M.J.; Olhero, A.; Antão, M.C.; Pina, M.F.; Guimarães, L.; Teixeira, J.; Afonso, M.J.; Delerue-Matos, C.; Chaminé, H.I. Assessment of Groundwater Contamination in an Agricultural Peri-Urban Area (NW Portugal): An Integrated Approach. *Environmental Earth Sciences* **2014**, *73*, 2881–2894, doi:10.1007/S12665-014-3297-3.
7. Rahmati, O.; Samani, A.N.; Mahmoodi, N.; Mahdavi, M. Assessment of the Contribution of N-Fertilizers to Nitrate Pollution of Groundwater in Western Iran (Case Study: Ghorveh–Dehgelan Aquifer). *Water Quality, Exposure and Health* **2014**, *7*:2 **2014**, *7*, 143–151, doi:10.1007/S12403-014-0135-5.
8. Lee, C.G.; Fletcher, T.D.; Sun, G. Nitrogen Removal in Constructed Wetland Systems. *Engineering in Life Sciences* **2009**, *9*, 11–22, doi:10.1002/ELSC.200800049.
9. Koskiaho, J.; Ekholm, P.; Rätty, M.; Riihimäki, J.; Puustinen, M. Retaining Agricultural Nutrients in Constructed Wetlands – Experiences under Boreal Conditions. *Ecological Engineering* **2003**, *20*, 89–103, doi:10.1016/S0925-8574(03)00006-5.
10. Lam, P.; Kuypers, M.M.M. Microbial Nitrogen Cycling Processes in Oxygen Minimum Zones. *Annual Review of Marine Science* **2011**, *3*, 317–345, doi:10.1146/annurev-marine-120709-142814.
11. Vidal, S.; Rocha, C.; Galvão, H. A Comparison of Organic and Inorganic Carbon Controls over Biological Denitrification in Aquaria. *Chemosphere* **2002**, *48*, 445–451, doi:10.1016/S0045-6535(02)00073-5.
12. Pang, Y.; Wang, J. Various Electron Donors for Biological Nitrate Removal: A Review. *Science of the Total Environment* **2021**, *794*, 148699, doi:10.1016/j.scitotenv.2021.148699.
13. Andalib, M.; Taher, E.; Donohue, J.; Ledwell, S.; Andersen, M.H.; Sangrey, K. Correlation between Nitrous Oxide (N₂O) Emission and Carbon to Nitrogen (COD/N) Ratio in Denitrification Process: A Mitigation Strategy to Decrease Greenhouse Gas Emission and Cost of Operation. *Water Science and Technology* **2018**, *77*, 426–438, doi:10.2166/wst.2017.558.
14. Shao, M.; Guo, L.; She, Z.; Gao, M.; Zhao, Y.; Sun, M.; Guo, Y. Enhancing Denitrification Efficiency for Nitrogen Removal Using Waste Sludge Alkaline Fermentation Liquid as External Carbon Source. *Environmental Science and Pollution Research* **2018**, *26*:5 **2018**, *26*, 4633–4644, doi:10.1007/S11356-018-3944-4.

15. Bezirgiannidis, A.; Marinakis, N.; Ntougias, S.; Melidis, P. Membrane Bioreactor Performance during Processing of a Low Carbon to Nitrogen Ratio Municipal Wastewater. *Environmental Processes 2018 5:1* **2018**, *5*, 87–100, doi:10.1007/S40710-018-0317-4.
16. Saeed, T.; Sun, G. A Review on Nitrogen and Organics Removal Mechanisms in Subsurface Flow Constructed Wetlands: Dependency on Environmental Parameters, Operating Conditions and Supporting Media. *Journal of Environmental Management* **2012**, *112*, 429–448.
17. Ji, B.; Zhao, Y.; Vymazal, J.; Mander, Ü.; Lust, R.; Tang, C. Mapping the Field of Constructed Wetland-Microbial Fuel Cell: A Review and Bibliometric Analysis. *Chemosphere* **2021**, *262*, 128366, doi:10.1016/j.chemosphere.2020.128366.
18. Gregory, K.B.; Bond, D.R.; Lovley, D.R. Graphite Electrodes as Electron Donors for Anaerobic Respiration. *Environmental Microbiology* **2004**, *6*, 596–604, doi:10.1111/j.1462-2920.2004.00593.x.
19. Dehghani, S.; Rezaee, A.; Hosseinkhani, S. Biostimulation of Heterotrophic-Autotrophic Denitrification in a Microbial Electrochemical System Using Alternating Electrical Current. *Journal of Cleaner Production* **2018**, *200*, 1100–1110, doi:10.1016/j.jclepro.2018.08.013.
20. Ding, A.; Zhao, D.; Ding, F.; Du, S.; Lu, H.; Zhang, M.; Zheng, P. Effect of Inocula on Performance of Bio-Cathode Denitrification and Its Microbial Mechanism. *Chemical Engineering Journal* **2018**, *343*, 399–407, doi:10.1016/j.cej.2018.02.119.
21. Kadier, A.; Jain, P.; Lai, B.; Kalil, M.S.; Kondaveeti, S.; Alabbosh, K.F.S.; Abu-Reesh, I.M.; Mohanakrishna, G. Biorefinery Perspectives of Microbial Electrolysis Cells (MECs) for Hydrogen and Valuable Chemicals Production through Wastewater Treatment. *Biofuel Research Journal* **2020**, *7*, 1128–1142, doi:10.18331/BRJ2020.7.1.5.
22. Sharma, M.; Alvarez-Gallego, Y.; Achouak, W.; Pant, D.; Sarma, P.M.; Dominguez-Benetton, X. Electrode Material Properties for Designing Effective Microbial Electrosynthesis Systems. *Journal of Materials Chemistry A* **2019**, *7*, 24420–24436, doi:10.1039/C9TA04886C.
23. Bonanni, P.S.; Schrott, G.D.; Robuschi, L.; Busalmen, J.P. Charge Accumulation and Electron Transfer Kinetics in *Geobacter Sulfurreducens* Biofilms. *Energy & Environmental Science* **2012**, *5*, 6188, doi:10.1039/c2ee02672d.
24. Pankratova, G.; Hederstedt, L.; Gorton, L. Extracellular Electron Transfer Features of Gram-Positive Bacteria. *Analytica Chimica Acta* **2019**, *1076*, 32–47, doi:10.1016/j.aca.2019.05.007.
25. Rannap, R.; Kaart, M.M.; Kaart, T.; Kill, K.; Uemaa, E.; Mander, Ü.; Kasak, K. Constructed Wetlands as Potential Breeding Sites for Amphibians in Agricultural Landscapes: A Case Study. *Ecological Engineering* **2020**, *158*, 106077, doi:10.1016/J.ECOLENG.2020.106077.
26. Mander, Ü.; Muring, T. Constructed Wetlands for Wastewater Treatment in Estonia. *Water Science and Technology* **1997**, *35*, 323–330, doi:10.2166/WST.1997.0228.
27. Kill, K.; Pärn, J.; Lust, R.; Mander, Ü.; Kasak, K. Treatment Efficiency of Diffuse Agricultural Pollution in a Constructed Wetland Impacted by Groundwater Seepage. *Water (Switzerland)* **2018**, *10*, doi:10.3390/w10111601.
28. Nguyen, V.K.; Park, Y.; Yu, J.; Lee, T. Bioelectrochemical Denitrification on Biocathode Buried in Simulated Aquifer Saturated with Nitrate-Contaminated Groundwater. *Environmental Science and Pollution Research* **2016**, *23*, 15443–15451, doi:10.1007/s11356-016-6709-y.

29. Yu, L.; Yuan, Y.; Chen, S.; Zhuang, L.; Zhou, S. Direct Uptake of Electrode Electrons for Autotrophic Denitrification by *Thiobacillus Denitrificans*. *Electrochemistry Communications* **2015**, *60*, 126–130, doi:10.1016/j.elecom.2015.08.025.
30. Pous, N.; Koch, C.; Colprim, J.; Puig, S.; Harnisch, F. Extracellular Electron Transfer of Biocathodes: Revealing the Potentials for Nitrate and Nitrite Reduction of Denitrifying Microbiomes Dominated by *Thiobacillus* Sp. *Electrochemistry Communications* **2014**, *49*, 93–97, doi:10.1016/j.elecom.2014.10.011.
31. KEGG PATHWAY: Nitrogen Metabolism – *Thiobacillus Denitrificans* Available online: https://www.genome.jp/kegg-bin/show_pathway?org_name=tbid&mapno=00910&mapscale=&show_description=hide (accessed on 9 January 2022).
32. Ceconet, D.; Devecseri, M.; Callegari, A.; Capodaglio, A.G. Effects of Process Operating Conditions on the Autotrophic Denitrification of Nitrate-Contaminated Groundwater Using Bioelectrochemical Systems. *Science of the Total Environment* **2018**, *613–614*, 663–671, doi:10.1016/j.scitotenv.2017.09.149.
33. Hutchinson, G.L.; Livingston, G.P. Use of Chamber Systems to Measure Trace Gas Fluxes. In *Agricultural Ecosystem Effects on Trace Gases and Global Climate Change*; John Wiley & Sons, Ltd, 2015; pp. 63–78.
34. Lofffield, N.; Flessa, H.; Augustin, J.; Beese, F. Automated Gas Chromatographic System for Rapid Analysis of the Atmospheric Trace Gases Methane, Carbon Dioxide, and Nitrous Oxide. *Journal of Environmental Quality* **1997**, *26*, 560–564, doi:10.2134/JEQ1997.00472425002600020030X.
35. Espenberg, M.; Truu, M.; Mander, Ü.; Kasak, K.; Nölvak, H.; Ligi, T.; Oopkaup, K.; Maddison, M.; Truu, J. Differences in Microbial Community Structure and Nitrogen Cycling in Natural and Drained Tropical Peatland Soils. *Scientific Reports* **2018** *8*:1 **2018**, *8*, 1–12, doi:10.1038/s41598-018-23032-y.
36. Kandeler, E.; Deiglmayr, K.; Tscherko, D.; Bru, D.; Philippot, L. Abundance of NarG, NirS, NirK, and NosZ Genes of Denitrifying Bacteria during Primary Successions of a Glacier Foreland. *Applied and Environmental Microbiology* **2006**, *72*, 5957, doi:10.1128/AEM.00439-06.
37. Wang, M.; Huang, G.; Zhao, Z.; Dang, C.; Liu, W.; Zheng, M. Newly Designed Primer Pair Revealed Dominant and Diverse Comammox AmoA Gene in Full-Scale Wastewater Treatment Plants. *Bioresour Technol* **2018**, *270*, 580–587, doi:10.1016/J.BIORTECH.2018.09.089.
38. Ruijter, J.M.; Ramakers, C.; Hoogaars, W.M.H.; Karlen, Y.; Bakker, O.; van den Hoff, M.J.B.; Moorman, A.F.M. Amplification Efficiency: Linking Baseline and Bias in the Analysis of Quantitative PCR Data. *Nucleic Acids Research* **2009**, *37*, e45–e45, doi:10.1093/nar/gkp045.
39. di Capua, F.; Pirozzi, F.; Lens, P.N.L.; Esposito, G. Electron Donors for Autotrophic Denitrification. *Chemical Engineering Journal* **2019**, *362*, 922–937, doi:10.1016/J.CEJ.2019.01.069.
40. Borin, M.; Tocchetto, D. Five Year Water and Nitrogen Balance for a Constructed Surface Flow Wetland Treating Agricultural Drainage Waters. *Science of The Total Environment* **2007**, *380*, 38–47, doi:10.1016/J.SCITOTENV.2006.12.039.
41. Jarvie, H.P.; King, S.M.; Neal, C. Inorganic Carbon Dominates Total Dissolved Carbon Concentrations and Fluxes in British Rivers: Application of the THINCARB Model – Thermodynamic Modelling of Inorganic Carbon in Freshwaters. *Science of The Total Environment* **2017**, *575*, 496–512, doi:10.1016/J.SCITOTENV.2016.08.201.

42. Pous, N.; Carmona-Martínez, A.A.; Vilajeliu-Pons, A.; Fiset, E.; Bañeras, L.; Trably, E.; Balaguer, M.D.; Colprim, J.; Bernet, N.; Puig, S. Bidirectional Microbial Electron Transfer: Switching an Acetate Oxidizing Biofilm to Nitrate Reducing Conditions. *Biosensors and Bioelectronics* **2016**, *75*, 352–358, doi:10.1016/j.bios.2015.08.035.
43. Thamdrup, B. New Pathways and Processes in the Global Nitrogen Cycle. *Annual Review of Ecology, Evolution, and Systematics* **2012**, *43*, 407–428, doi:10.1146/annurev-ecolsys-102710-145048.
44. Gregoire, K.P.; Glaven, S.M.; Herve, J.; Lin, B.; Tender, L.M. Enrichment of a High-Current Density Denitrifying Microbial Biocathode. *Journal of The Electrochemical Society* **2014**, *161*, H3049–H3057, doi:10.1149/2.0101413jes.
45. Safari, M.; Rezaee, A.; Ayati, B.; Jonidi-Jafari, A. Bio-Electrochemical Reduction of Nitrate Utilizing MWCNT Supported on Carbon Base Electrodes: A Comparison Study. *J Taiwan Inst Chem Eng* **2014**, *45*, 2212–2216, doi:10.1016/j.jtice.2014.05.006.
46. Chen, D.; Yang, K.; Wang, H. High Nitrate Removal by Autohydrogenotrophic Bacteria in a Biofilm-Electrode Reactor. *Desalination and Water Treatment* **2015**, *55*, 1316–1324, doi:10.1080/19443994.2014.925837.
47. Rezaee, A.; Safari, M.; Hossini, H. Bioelectrochemical Denitrification Using Carbon Felt/Multiwall Carbon Nanotube. *Environmental Technology* **2015**, *36*, 1057–1062, doi:10.1080/09593330.2014.974680.
48. Qambrani, N.A.; Oh, S.E. Effect of Dissolved Oxygen Tension and Agitation Rates on Sulfur-Utilizing Autotrophic Denitrification: Batch Tests. *Applied Biochemistry and Biotechnology* **2013**, *169*, 181–191, doi:10.1007/s12010-012-9955-6.
49. Gómez, M. Effect of Dissolved Oxygen Concentration on Nitrate Removal from Groundwater Using a Denitrifying Submerged Filter. *Journal of Hazardous Materials* **2002**, *90*, 267–278, doi:10.1016/S0304-3894(01)00353-3.
50. Zhou, S.; Huang, S.; He, J.; Li, H.; Zhang, Y. Electron Transfer of Pseudomonas Aeruginosa CP1 in Electrochemical Reduction of Nitric Oxide. *Bioresource Technology* **2016**, *218*, 1271–1274, doi:10.1016/j.biortech.2016.07.010.
51. Ceballos-Escalera, A.; Pous, N.; Chiluíza-Ramos, P.; Korth, B.; Harnisch, F.; Bañeras, L.; Balaguer, M.D.; Puig, S. Electro-Bioremediation of Nitrate and Arsenite Polluted Groundwater. *Water Research* **2021**, *190*, 116748, doi:10.1016/j.watres.2020.116748.
52. Gimkiewicz, C.; Harnisch, F. Waste Water Derived Electroactive Microbial Biofilms: Growth, Maintenance, and Basic Characterization. *Journal of Visualized Experiments* **2013**, 50800, doi:10.3791/50800.
53. Kondaveeti, S.; Min, B. Nitrate Reduction with Biotic and Abiotic Cathodes at Various Cell Voltages in Bioelectrochemical Denitrification System. *Bioprocess and Biosystems Engineering* **2013**, *36*, 231–238, doi:10.1007/s00449-012-0779-0.
54. Li, P.; Wang, Y.; Zuo, J.; Wang, R.; Zhao, J.; Du, Y. Nitrogen Removal and N₂O Accumulation during Hydrogenotrophic Denitrification: Influence of Environmental Factors and Microbial Community Characteristics. *Environmental Science and Technology* **2017**, *51*, 870–879, doi:10.1021/acs.est.6b00071.
55. Al-Mamun, A.; Baawain, M.S. Accumulation of Intermediate Denitrifying Compounds Inhibiting Biological Denitrification on Cathode in Microbial Fuel Cell. *Journal of Environmental Health Science and Engineering* **2015**, *13*, 81, doi:10.1186/s40201-015-0236-5.

56. Su, W.; Zhang, L.; Li, D.; Zhan, G.; Qian, J.; Tao, Y. Dissimilatory Nitrate Reduction by *Pseudomonas Alcaliphila* with an Electrode as the Sole Electron Donor. *Biotechnology and Bioengineering* **2012**, *109*, 2904–2910, doi:10.1002/BIT.24554.
57. Hallin, S.; Philippot, L.; Löffler, F.E.; Sanford, R.A.; Jones, C.M. Genomics and Ecology of Novel N₂O-Reducing Microorganisms. *Trends in Microbiology* **2018**, *26*, 43–55, doi:10.1016/J.TIM.2017.07.003.
58. Zhou, M.; Wang, H.; Hassett, D.J.; Gu, T. Recent Advances in Microbial Fuel Cells (MFCs) and Microbial Electrolysis Cells (MECs) for Wastewater Treatment, Bioenergy and Bioproducts. *Journal of Chemical Technology and Biotechnology* **2013**, *88*, 508–518, doi:10.1002/jctb.4004.
59. Zhao, Y.; Collum, S.; Phelan, M.; Goodbody, T.; Doherty, L.; Hu, Y. Preliminary Investigation of Constructed Wetland Incorporating Microbial Fuel Cell: Batch and Continuous Flow Trials. *Chemical Engineering Journal* **2013**, *229*, 364–370, doi:10.1016/J.CEJ.2013.06.023.
60. Liu, S.; Song, H.; Wei, S.; Yang, F.; Li, X. Bio-Cathode Materials Evaluation and Configuration Optimization for Power Output of Vertical Subsurface Flow Constructed Wetland – Microbial Fuel Cell Systems. *Bioresource Technology* **2014**, *166*, 575–583, doi:10.1016/J.BIORTECH.2014.05.104.
61. Villaseñor Camacho, J.; del Carmen Montano Vico, M.; Andrés, M.; Rodrigo, R.; Jesús Fernández Morales, F.; Cañizares Cañizares, P. Energy Production from Wastewater Using Horizontal and Vertical Subsurface Flow Constructed Wetlands. *Environmental Engineering and Management Journal* **2014**, *13*, 2517–2523.
62. Corbella, C.; Garfí, M.; Puigagut, J. Vertical Redox Profiles in Treatment Wetlands as Function of Hydraulic Regime and Macrophytes Presence: Surveying the Optimal Scenario for Microbial Fuel Cell Implementation. *Science of The Total Environment* **2014**, *470–471*, 754–758, doi:10.1016/J.SCITOTENV.2013.09.068.
63. Yang, Y.; Zhao, Y.; Tang, C.; Xu, L.; Morgan, D.; Liu, R. Role of Macrophyte Species in Constructed Wetland-Microbial Fuel Cell for Simultaneous Wastewater Treatment and Bioenergy Generation. *Chemical Engineering Journal* **2020**, *392*, 123708, doi:10.1016/J.CEJ.2019.123708.
64. Wang, Q.; Lv, R.; Rene, E.R.; Qi, X.; Hao, Q.; Du, Y.; Zhao, C.; Xu, F.; Kong, Q. Characterization of Microbial Community and Resistance Gene (*CzcA*) Shifts in up-Flow Constructed Wetlands-Microbial Fuel Cell Treating Zn (II) Contaminated Wastewater. *Bioresource Technology* **2020**, *302*, 122867, doi:10.1016/J.BIORTECH.2020.122867.
65. Ge, X.; Cao, X.; Song, X.; Wang, Y.; Si, Z.; Zhao, Y.; Wang, W.; Tesfahunegn, A.A. Bioenergy Generation and Simultaneous Nitrate and Phosphorus Removal in a Pyrite-Based Constructed Wetland-Microbial Fuel Cell. *Bioresource Technology* **2020**, *296*, 122350, doi:10.1016/J.BIORTECH.2019.122350.
66. Guadarrama-Pérez, O.; Gutiérrez-Macías, T.; García-Sánchez, L.; Guadarrama-Pérez, V.H.; Estrada-Arriaga, E.B. Recent Advances in Constructed Wetland-Microbial Fuel Cells for Simultaneous Bioelectricity Production and Wastewater Treatment: A Review. *International Journal of Energy Research* **2019**, *43*, 5106–5127, doi:10.1002/ER.4496.
67. Yakar, A.; Türe, C.; Türker, O.C.; Vymazal, J.; Saz, Ç. Impacts of Various Filtration Media on Wastewater Treatment and Bioelectric Production in Up-Flow Constructed Wetland Combined with Microbial Fuel Cell (UCW-MFC). *Ecological Engineering* **2018**, *117*, 120–132, doi:10.1016/J.ECOLENG.2018.03.016.
68. Päikesepaneelide Hinna- Ja Effektiivsuse Kalkulaator Available online: <https://paikesepaneel.ee/> (accessed on 24 May 2022).

SUMMARY IN ESTONIAN

Bioelektrokeemilised süsteemid nitraadi võimendatud eraldamiseks väikse elektronidoonori sisaldusega veest

Intensiivne põlluharimine, väetiste liigkasutamine ja puhastamata reovee juhtimine keskkonda põhjustavad kogu maailmas pinna- ja põhjavee hajusreostust [1,2]. Üks reostust tekitav ühend on nitraat (NO_3^-), mille suur kontsentratsioon pinnavees põhjustab eutrofeerumist ja võib seeläbi viia elurikkuse vähenemiseni veekogus [3]. Uuringud on näidanud, et paljudes riikides, sealhulgas Portugalis, Iraanis ja Prantsusmaal, ületab NO_3^- kontsentratsioon põhjavees 50 mg NO_3^-/l piirnормi [4–7]. Kui NO_3^- kontsentratsioon vees ületab 50 mg NO_3^-/l piiri, siis on Maailma Terviseorganisatsiooni liigituse alusel tegemist joogikõlbmatu veega, kuna suurtes kogustes NO_3^- tarbimine võib põhjustada methemoglobineemiat või seedetrakti vähki [1,3]. Seetõttu on oluline arendada eri tehnoloogiaid, mille abil saaks veest NO_3^- eemaldada.

Olenevalt puhastatava vee omadustest võivad veepuhastussüsteemi ülesehitus ja juhtimine märkimisväärselt erineda. Lämmastikurikka vee puhastamiseks on rajatud tehismärgalasid (CW), kus saasteained eemaldatakse kasvava taimestiku ja mikroobsete protsesside abil [8,9].

Enamikul juhtudel eemaldatakse veest lämmastik mitmesuguste mikroobide abil, mis viivad läbi eri protsesse, näiteks nitrifikatsiooni, denitrifikatsiooni või anaeroobset ammooniumi oksüdatsiooni [8]. Siinse doktoritöö keskmes on denitrifikatsioon, mille käigus muudetakse NO_3^- lämmastikuks (N_2) [10]. Denitrifikatsioon võib toimuda kas heterotroofselt või autotroofselt, olenevalt keskkonnas leiduvatest ühenditest ja bakteritest [11]. Heterotroofse denitrifikatsiooni korral kasutavad mikroobid orgaanilisi ühendeid elektronidoonorite ja süsinikuallikana [12]. Autotroofse denitrifikatsiooni puhul tarvitavad mikroobid väävlit, vesinikku (H_2) või muid anorgaanilisi ühendeid elektronidoonoritena ja anorgaanilist süsinikku, näiteks süsinikdioksiidi (CO_2) või karbonaati, kasvuku vajaliku süsiniku allikana [12].

Elektronidoonorite väike kontsentratsioon on üks peamisi denitrifikatsiooni takistavaid tegureid [13]. Kui elektronidoonorite kontsentratsioon on keskkonnas väike, siis hakkavad kogunema denitrifikatsiooniga seotud vaheühendid, nagu nitrit (NO_2^-) või dilämmastikoksiid (N_2O) [13]. NO_2^- akumulatsioon keskkonnas pärsib denitrifikatsiooniprotsessi, mistõttu vee puhastamise efektiivsus väheneb, N_2O on tuntud kui kasvuhoonegaas, mis põhjustab kliimasoojenemist. Tagamaks, et vee puhastamine denitrifikatsiooni toel toimib optimaalselt ja mõju kliimale on minimeeritud, on oluline, et süsteemis oleks piisaval määral elektronidoonoreid. Sageli lisatakse reoveepuhastusjaamades elektronidoonorite osakaalu suurendamiseks orgaanilist süsinikku, näiteks metanooli või etanooli [14,15]. CWdes kasutatakse orgaanilise süsiniku lisaallikana puidumultši, aktiiv- või biosütti [16]. Kui süsteemi varustatakse orgaanilise süsinikuga, aitab see eemaldada NO_3^- , kuid seda lähenemisviisi ei saa kasutada igas olukorras. Näiteks

orgaanilise süsiniku lisamine põhjavee puhastamiseks võib põhjustada sekundaarset reostust ja muuta vee seeläbi joogikõlbmatuks.

Mikroobseid kütuseelemente (MFC) on uuritud juba aastakümneid eesmärgiga toota energiat ja ühtlasi suurendada puhastusefektiivsust [17]. Kuid olukorras, kus elektronidoonorite kontsentratsioon puhastatavas vees on väike, ei ole MFCd võimelised NO_3^- puhastusefektiivsust suurendama. Seetõttu on vaja teistsugust lähenemisviisi. Varasemad uuringud on näidanud, et mõned mikroorganismid, näiteks *Geobacter*'i-liigid, võivad tarbida elektrone otse elektrodidelt ja kasutada neid elektrone NO_3^- redutseerimiseks [18]. Seetõttu on tõenäoline, et kui MFCd kasutatakse pöördrežiimis, s.o elektrolüüserina – ehk siis elektri tootmise asemel hoopis rakendatakse elektrit –, on võimalik viia läbi mittespontaanseid reaktsioone. Selliseid süsteeme nimetatakse mikroobseteks elektrosünteesirakkudeks (MES). Viimastega seoses on tehtud arvukalt uuringuid, et hinnata eri protsesside läbiviimise võimalikkust, või uuritud seda, kuidas oleks võimalik suurendada protsesside efektiivsust, muutes reaktori disaini [19–22]. Lisaks on tehtud uuringuid, milles kirjeldatakse mikroobide ja elektrodide interaktsioone. Sellest hoolimata pole mainitud tehnoloogiat veel laialdaselt kasutama hakatud [23,24].

Mikroorganismide varustamine elektronidega elektrodide vahendusel, et saavutada parem NO_3^- puhastusefektiivsus vees, on suure potentsiaaliga. Seeläbi saaks vähendada eespool mainitud keskkonnaprobleeme ja puhastada vett ka olukordades, kus orgaanilisi süsinikuühendeid ei ole võimalik lisada. Seetõttu tuleks seda tehnoloogiat ja selle rakendamise võimalusi uurida ning sellest lähtudes on seatud ka sinise doktoritöö eesmärgid:

- saavutada stabiilne NO_3^- ärastus denitrifikatsiooni teel mikroobses elektrosünteesireaktoris (MESR) (artiklid II ja III);
- leida optimaalne tööelektroodi (WE) potentsiaal, kus Faraday efektiivsus on suurim ja ammoniumi (NH_4^+) või denitrifikatsiooniga seotud vaheühendeid ei akumulereuks (artikkel III);
- hinnata MESRi kasutamise mõju kasvuhoonegaaside (KHG) emissioonile (artikkel II);
- anda ülevaade, kuidas elektrodide kasutamine mõjutab lämmastiku-aineringe funktsionaalsete geenide arvukust (artikkel III);
- hinnata avaveelise tehismärgala efektiivsust põllumajandusliku hajureostuse vähendamisel põhjamaises kliimas (artikkel I) ja MESRi integreerimise võimalikkust valitud tehismärgalas;
- uurida, kas on avaldatud artikleid, mille puhul oleks tehismärgalas integreeritud mikrobioloogilist kütuseelementi (CW-MFC) edukalt kasutatud selleks, et eemaldada NO_3^- veest, milles on väike elektronidoonorite kontsentratsioon (artikkel IV).

Eesmärkidest lähtudes seati järgmised hüpoteesid:

1. MESRi vahendusel on võimalik vahetult varustada mikroorganisme elektroni-dega, asendades seeläbi elektronidoonoreid.
2. Denitrifikatsiooni efektiivsust mõjutab kasutatav WE potentsiaal.
3. MESRi saab kasutada NO_3^- eemaldamiseks väikse orgaanilise süsiniku kontsentratsiooniga veest, kus muidu NO_3^- ärastust ei toimu.

Doktoritöö käigus hinnati Tartumaal Uhti külas Vända tehismärgala (CW) puhastusefektiivsust. Tegemist on kaheosalise CWga, mille efektiivne pindala on u 0,2 ha. Veeproove koguti kaks korda nädalas alates 2017. aasta märtsist ja uuringuperioodil võeti kokku 132 proovi. Iga kord koguti proovid mõlema CW osa sisse- ja väljavooluavade juurest ning kord kuus võeti proovid ka piesomeetritest, mis olid paigaldatud kahte CW osa ühendava kraavi äärtele. Mõõtmiste käigus selgus, et Vända CWs oli NO_3^- ärastusefektiivsus $-31,6\%$, mis tähendab seda, et NO_3^- kontsentratsioon vees kasvas 4,1-lt 5,4-le mg N- NO_3^- /l. See oli põhjustatud kahe aspekti koosmõjust: NO_3^- -rikka põhjavee sissetungist CWsse ja väiksest NO_3^- ärastuskiirusest. Orgaanilise süsiniku ja NO_3^- suhtest, mis oli 11 : 1, võib selgelt järeldada, et väike NO_3^- ärastuskiirus on põhjustatud ka väiksest elektronidoonorite kontsentratsioonist, mis on pinnaveekogude puhul tavaline [13].

Selleks et hinnata, kas MESRi saaks kasutada NO_3^- eemaldamiseks veest, milles on väike elektronidoonorite kontsentratsioon, valmistati kaks kahekambrilist reaktorit, mille koguruumala oli 5,86 l. Esimeses katses otsustati kahekambrilise reaktori kasuks, kuna abielektroodil (CE) tekib elektrolüüsi käigus hapnik (O_2), mis segab denitrifikatsiooniprotsessi. Kuna mõlemad kambrid olid üksteisest prootonvahetusmembraani (PEM) abil eraldatud, ei pääsenud CE-l tekkiv O_2 WE-kambrisse, kus kavatseti läbi viia denitrifikatsiooni. Esimeses katses kasutati WE valmistamiseks süsinikkiudriiet mõõduga 20×61 cm ja CE valmistati süsinikpulbriga kaetud roostevabast terasvõrgust mõõduga 20×16 cm. Kambrites oleva elektrolüüdi segamiseks kasutati eraldi pumpasid ning reaktorid olid varustatud kahe avaga, mille kaudu sai võtta gaasi- ja veeproove.

Pärast reaktorite kokkupanemist täideti need sünteetilise reoveega, mis oli valmistatud kraaniveest, kuhu oli lisatud 4,64 g/l Na_2HPO_4 , 1,75 g/l NaH_2PO_4 , 1,39 g/l NaHCO_3 ja 0,165 g/l KNO_3 . Seejärel juhiti reaktorisse N_2 , et tagada väike O_2 kontsentratsioon katse alguses. WE inokuleerimiseks lisati WE-kambrisse reoveepuhastist võetud muda ja pärast 7päevast inokuleerimist WE potentsiaalil +394 standardvesinikelektroodi (SHE) suhtes kasutati denitrifikatsiooni toetamiseks potentsiaali -306 mV vs. SHE.

Katse kestis kokku 45 päeva ja selle käigus selgus, et MESR suutis NO_3^- ärastuskiirust suurendada 0,7-lt 1,4-le mg N- NO_3^- / ($1 \times$ päev). Samal ajal oli keskmine N_2O emissioon MESRis ($-0,64$ mg N / ($\text{m}^2 \times \text{h}$)) väiksem kui kontrollreaktoris ($-0,01$ mg N / ($\text{m}^2 \times \text{h}$)). Hoolimata NO_3^- ärastusefektiivsuse suurenemisest oli kasv liiga väike. Kahekambrilise MESRi kasutamine suutis

hoida CE-1 toodetud hapniku WE-kambrist eemal. Kuid see põhjustas kõikumist lahuse pHs, mida oli vaja pidevalt reguleerida. Viimane probleem oli rooste-
vabast terasest valmistatud CE, mis katse lõpuks oli niivõrd korrodeerunud, et
ühendus potentsiaastaadi ja elektroodi vahel katkes.

Teises katses otsustati kasutada ühekambrilist MESRi. Selleks eemaldati
varem ehitatud reaktoritelt PEMi kandev rakis koos membraaniga. Et vähendada
hapniku eraldumist CE-1, vahetati elektroodide asukohad ning selle tulemusena
oli CE mõõt 20×61 ja WE mõõt 20×16 . Lisaks kasutati teises katses mõlema
elektroodi valmistamiseks grafiitvilti. Ühenduste valmistamiseks tarvitati titaan-
traati, tagamaks, et katse käigus materjal ei korrodeeru ning ühendus potentsio-
staadi ja elektroodi vahel ei katke. Kuna grafiitvilt on rabe materjal, liimiti titaan-
traat grafiitvildi külge epoksü- ja süsinikpulbrit sisaldava liimi seguga, mis on
vees lahustumatu ning ühtlasi juhib elektrit. Reaktorid täideti sarnaselt eelmise
katsega sünteetilise reoveega, kuid inokuleerimiseks kasutati bakteri *Thiobacillus*
denitrificans kultuuri, et kontrollida, kas see sobib NO_3^- ärastamiseks. Reakto-
ritega tehti hulganisti katseid, proovides läbi erinevaid WE potentsiaale, mille
tulemusena kestis kogu eksperiment kokku peaaegu kaks aastat.

Ühekambrilise MESRi kasutamisel püsis pH stabiilsena 7,3 lähedal ega vaja-
nud kordagi reguleerimist. Ka CE-1 tekkiva O_2 hulk oli niivõrd väike, et ei suuren-
danud reaktoris lahustunud hapniku kontsentratsiooni. Katse käigus prooviti läbi
erinevaid WE potentsiaale, alustades suurematest potentsiaaliväärtustest
(-320 mV vs. SHE) ja liikudes üha väiksemate potentsiaaliväärtuste poole. Alles
WE potentsiaalil -756 mV vs. SHE hakkas NO_3^- kontsentratsioon märgatavalt
väheneda. Seejuures käitus ka voolutihedus pärast protsessi käivitamist loogiliselt
ehk voolutihedus $|j|$ oli tunduvalt väiksem, kui veest oli kogu NO_3^- eemaldatud.
Kontrollreaktoris samal ajal aga NO_3^- kontsentratsioon ei muutunud, seega võib
kindlalt väita, et tegemist oli MESRi abil elluviidud protsessiga. Katse käigus
selgus, et optimaalne WE potentsiaal on -656 mV vs. SHE, kus NO_3^- ärastus-
kiirus oli $3,8 \pm 1,2$ mg N- NO_3^- / ($l \times$ päev).

Võrreldes CEga oli nitriti reduktaasi ja dilämmastikoksiidi reduktaasi geenide
arvukus WE-1 palju suurem, mis näitab, et NO_3^- ärastus toimus denitrifikatsiooni
kaudu. WE potentsiaalil -756 mV vs. SHE esines ka NH_4^+ kontsentratsiooni
suurenemine, mis tähendab, et väiksemate WE potentsiaalide korral võib dissimi-
latoorne nitraadi redutseerimine ammooniumiks konkureerida ka denitrifikat-
siooniga. Suurematel WE potentsiaalidel NH_4^+ kontsentratsioon aga vähenes, mis
tähendab seda, et MESRi abil on võimalik ka NH_4^+ veest eemaldada. Denitri-
fikatsiooniga seotud vaheühendeid, näiteks NO_2^- akumulatsiooni, selles katses ei
esinenud. Eelmainitud tegurite tõttu on oluline leida MESRiga töötamiseks õige
WE potentsiaal, mille puhul on saavutatud tasakaal soovitud protsesside toimi-
mise ja soovimatute ühendite vältimise vahel ning energiatarbelts kõige efek-
tiivsem olukord.

MESRi katsega saavutatud NO_3^- ärastuskiiruse põhjal peaks Vända CWs NO_3^-
täielikuks eemaldamiseks kasutama WEd kogupindalaga 964 m². Kuna Vända
CWs on probleem ka põhjavee sissetungiga, tuleks MESR paigutada väljavoolu-
ava lähedusse. Arvutuste põhjal on CW väljavooluosa MESRi mahutamiseks

piisavalt suur. Tuginedes katse käigus leitud voolutihedusele, peab kasutatava elektrivooluallika minimaalne väljundvoolu tugevus olema vähemalt 434 A. Mõistlik on jagada WE mitmesse sektsiooni ning juhtida neid eri vooluallikatega, et tagada ühtlasem pingeaotus. Otstarbekas on aga enne nii suure projekti rakendamist teha mõned pilootuuringud, et leida parim viis, kuidas elektroodid peaksid olema paigutatud, ning hinnata, kuidas voolukiirus ja madalam veetemperatuur MESRis toimuvat NO_3^- ärastuskiirust mõjutavad.

Kuna MESR vajab NO_3^- ärastamiseks energiat, analüüsi katsete tegemise ajal ka kirjandust, milles on uuritud CW-MFCd. Analüüsi tulemusena valmis ülevaade, millised on praegusajal aktuaalsed teemad ja kui kaugele on selles valdkonnas jõutud. Võtmesõnade alusel tulid välja järgmised põhiteemad: bioelektri tootmise efektiivsus, mikrobioloogia, probleemsete saasteainete eemaldamine ja traditsiooniliste saasteainete eemaldamise efektiivsus. Aja jooksul on uurimisteemad muutunud spetsiifilisemaks ning keskenduvad eri taimede, substraatide, elektroodimaterjalide, hüdrauliliste režiimide ja reaktori disaini kasutamisele, samuti sellele, kuidas need mõjutavad saasteainete puhastamise efektiivsust ja elektritootmist. Praegused CW-MFC-süsteemid on suuruselt aga piloot- või laborikatsete tasemel ning artikleid, kus CW-MFCd saaks kasutada NO_3^- eemaldamiseks madala elektronidoonorite kontsentratsiooni korral, ei leitud. Ka siinses doktoritöös käsitletud MESRi puhul on tegemist laborikatsega ning üldiselt on uuritavad aspektid samad mis MFCdel. Mõlema süsteemi puhul on keskne komponent mikroorganismide ja elektroodide interaktsioon ning seetõttu saab MFCga seotud avastusi rakendada ka MESRide puhul. Üks ühisjoon on näiteks materjal, millest elektroode valmistatakse. Levinuimad on süsinikust tehtud elektroodid, mis on end tõestanud bakteritele sobivate kasvukohtadena.

MESRiga tehtud katsete käigus saavutatud tulemuste põhjal võib öelda, et MES on paljulubav tehnoloogia denitrifikatsiooni tõhustamiseks olukordades, kus elektronidoonori kontsentratsioon on väike. Ja ka Vända CW võiks olla üks võimalik kandidaat, kus saaks MESRi rakendada, kuid enne suurema projekti alustamist tuleks teha veel pilootuuringuid.

ACKNOWLEDGEMENTS

First, I would like to thank my supervisors Jaak Nerut, Ülo Mander and Kuno Kasak for giving me the opportunity to work on such an interesting topic. We all know it was not easy to reach the goal, and sometimes it seemed as though process would never start, but after all, it looks like we made it. There is still much to discover, but at least the hard part, taking the first step towards the right direction, is done. Additionally, a big thank you to Alar Teemusk, Mae Uri, Kristel Kroon and Triinu Visnapuu, who helped me a lot with different chemical analyses throughout the years.

And of course, my eternal gratitude goes to my family, who have always been there for me during this rollercoaster ride... Thank you!

This research was supported by the Estonian Research Council (grants no. PSG631, PSG714, PRG352) and by the European Union (EU) through the European Regional Development Fund (Centre of Excellence EcolChange (TK131) and ‘Advanced materials and high-technology devices for energy recuperation systems (TK141)’).

PUBLICATIONS

CURRICULUM VITAE

Name: Rauno Lust
Date of birth: 14.05.1990
E-mail: Raunolust@live.com

Education:

2017–2022 University of Tartu, PhD in Environmental Technology
2014–2017 University of Tartu, MSc in Environmental Technology, *cum laude*
2011–2014 University of Tartu, BSc in Environmental Technology
2007–2011 Rakvere adult high school
1997–2007 Rakvere basic school

Work experience:

2021–... Republic of Estonia Environment Agency, Environmental analysis and reporting department, leading specialist

Research interests:

Environmental technology, bioelectrochemistry, biotechnology

Publications:

Kill, K.; Pärn, J.; Lust, R.; Mander, Ü.; Kasak, K. Treatment Efficiency of Diffuse Agricultural Pollution in a Constructed Wetland Impacted by Groundwater Seepage. *Water* 2018, 10, 1601. <https://doi.org/10.3390/w10111601>

Lust, R.; Nerut, J.; Kasak, K.; Mander, Ü. Enhancing Nitrate Removal from Waters with Low Organic Carbon Concentration Using a Bioelectrochemical System – A Pilot-Scale Study. *Water* 2020, 12, 516. <https://doi.org/10.3390/w12020516>

Gadegaonkar, S.S.; Philippon, T.; Rogińska, J.M.; Mander, Ü.; Maddison, M.; Etienne, M.; Barrière, F.; Kasak, K.; Lust, R.; Espenberg, M. Effect of Cathode Material and Its Size on the Abundance of Nitrogen Removal Functional Genes in Microcosms of Integrated Bioelectrochemical-Wetland Systems. *Soil Syst.* 2020, 4, 47. <https://doi.org/10.3390/soilsystems4030047>

Ji, B.; Zhao, Y.; Vymazal, J.; Mander, Ü.; Lust, R.; Tang, C. (2021). Mapping the field of constructed wetland-microbial fuel cell: A review and bibliometric analysis. *Chemosphere*, 262. <https://doi.org/10.1016/j.chemosphere.2020.128366>

Conference presentations:

Lust, R. (June 2019). *Microbial Electrosynthesis Cells For the Enhancement of Purification Processes In Treatment Wetlands*. Oral presentation at the 8th International Symposium on Wetland Pollutant Dynamics and Control (WETPOL 2019). Aarhus, Denmark.

Lust, R. (December 2019). *Microbial Electrosynthesis Cells For the Enhancement of Purification Processes In Treatment Wetlands*. Oral presentation at the 2019 International Workshop on Constructed Wetland – Microbial Fuel Cell Technology (IWonCW-MFC2019). Xi'an, China.

Courses:

2018–2021 Environmental Management Systems and Auditing (LOOM.02.162).

ELULOOKIRJELDUS

Nimi Rauno Lust
Sünniaeg: 14.05.1990
E-mail: Raunolust@live.com

Haridus:

2017–2022 Tartu Ülikool, PhD keskkonnatehnoloogias
2014–2017 Tartu Ülikool, MSc keskkonnatehnoloogias, *cum laude*
2011–2014 Tartu Ülikool, BSc keskkonnatehnoloogias
2007–2011 Rakvere Täiskasvanute Gümnaasium
1997–2007 Rakvere Põhikool

Töökogemus:

2021–... Keskkonnaagentuur, Keskkonnanalüüsi ja aruandluse osakond, juhtivspetsialist

Uurimisvaldkonnad:

Keskkonnatehnoloogia, bioelektrokeemia, biotehnoloogia

Publikatsioonid:

Kill, K.; Pärn, J.; Lust, R.; Mander, Ü.; Kasak, K. Treatment Efficiency of Diffuse Agricultural Pollution in a Constructed Wetland Impacted by Groundwater Seepage. *Water* 2018, 10, 1601. <https://doi.org/10.3390/w10111601>

Lust, R.; Nerut, J.; Kasak, K.; Mander, Ü. Enhancing Nitrate Removal from Waters with Low Organic Carbon Concentration Using a Bioelectrochemical System – A Pilot-Scale Study. *Water* 2020, 12, 516. <https://doi.org/10.3390/w12020516>

Gadegaonkar, S.S.; Philippon, T.; Rogińska, J.M.; Mander, Ü.; Maddison, M.; Etienne, M.; Barrière, F.; Kasak, K.; Lust, R.; Espenberg, M. Effect of Cathode Material and Its Size on the Abundance of Nitrogen Removal Functional Genes in Microcosms of Integrated Bioelectrochemical-Wetland Systems. *Soil Syst.* 2020, 4, 47. <https://doi.org/10.3390/soilsystems4030047>

Ji, B.; Zhao, Y.; Vymazal, J.; Mander, Ü.; Lust, R.; Tang, C. (2021). Mapping the field of constructed wetland-microbial fuel cell: A review and bibliometric analysis. *Chemosphere*, 262. <https://doi.org/10.1016/j.chemosphere.2020.128366>

Suulised ettekanded konverentsidel:

Lust, R. (June 2019). *Microbial Electrosynthesis Cells For the Enhancement of Purification Processes In Treatment Wetlands*. The 8th International Symposium on Wetland Pollutant Dynamics and Control (WETPOL 2019). Aarhus, Taani.

Lust, R. (December 2019). *Microbial Electrosynthesis Cells For the Enhancement of Purification Processes In Treatment Wetlands*. 2019 International Workshop on Constructed Wetland – Microbial Fuel Cell Technology (IWonCW-MFC2019). Xi'an, Hiina.

Kursused:

2018–2021 Keskkonnajuhtimine ja keskkonnaaudit (LOOM.02.162).

DISSERTATIONES TECHNOLOGIAE CIRCUMIECTORUM UNIVERSITATIS TARTUENSIS

1. **Sille Teiter.** Emission rates of N₂O, N₂, CH₄ and CO₂ in riparian grey alder forests and subsurface flow constructed wetlands. Tartu, 2005, 134 p.
2. **Kaspar Nurk.** Relationships between microbial characteristics and environmental conditions in a horizontal subsurface flow constructed wetland for wastewater treatment. Tartu, 2005, 123 p.
3. **Märt Öövel.** Performance of wastewater treatment wetlands in Estonia. Tartu, 2006, 148 p.
Sergei Yurchenko. Determination of some carcinogenic contaminants in food. Tartu, 2006, 143 p. Published in *Dissertation Chimicae Universitatis Tartuensis*, 51.
4. **Alar Noorvee.** The applicability of hybrid subsurface flow constructed wetland systems with re-circulation for wastewater treatment in cold climates. Tartu, 2007, 117 p.
Ülle Jõgar. Conservation and restoration of semi-natural floodplain meadows and their rare plant species. Tartu, 2008, 99 p. Published in *Dissertation Biologicae Universitatis Tartuensis*, 139.
5. **Christina Vohla.** Phosphorus removal by various filter materials in subsurface flow constructed wetlands. Tartu, 2008, 103 p.
6. **Martin Maddison.** Dynamics of phytomass production and nutrient standing stock of cattail and its use for environment-friendly construction. Tartu, 2008, 87 p.
7. **Marika Truu.** Impact of land use on microbial communities in Estonian soils. Tartu, 2008, 126 p.
8. **Elar Põldvere.** Removal of organic material, nitrogen and phosphorus from wastewater in hybrid subsurface flow constructed wetlands. Tartu, 2009, 107 p.
9. **Margit Kõiv.** Treatment of landfill leachate and municipal wastewater in subsurface flow filters using mineralized peat and hydrated oil shale ash. Tartu, 2010, 147 p.
10. **Jaanis Juhanson.** Impact of phytoremediation and bioaugmentation on the microbial community in oil shale chemical industry solid waste. Tartu, 2010, 95 p.
Aare Selberg. Evaluation of environmental quality in Northern Estonia by the analysis of leachate. Tartu, 2010, 117 p. Published in *Dissertation Chimicae Universitatis Tartuensis*, 99.
11. **Riho Mõtlep.** Composition and diagenesis of oil shale industrial solid wastes. Tartu, 2010, 127 p.
12. **Igor Zaytsev.** Bioaugmentation in LWA-filled horizontal subsurface flow filters for wastewater treatment: Impact of flow regime, temperature and donor system Tartu, 2010, 97 p.

13. **Siiri Velling.** Microbial BOD biosensor for wastewater analysis. Tartu, 2011, 79 p.
14. **Riina Lepik.** Biodegradability of phenolic compounds as single and mixed substrates by activated sludge. Tartu, 2011, 153 p.
15. **Liis Marmor.** Ecology and bioindicative value of epiphytic lichens in relation to air pollution and forest continuity. Tartu, 2011, 98 p.
16. **Martin Liira.** Active filtration of phosphorus in Ca-rich hydrated oil shale ash: precipitation mechanisms and recovery. Tartu, 2012, 84 p.
17. **Kristjan Karabelnik.** Advanced design and management of hybrid constructed wetlands: environmental and water purification effects. Tartu, 2012, 128 p.
18. **Hiie Nõlvak.** Influence of qPCR workflow on target gene enumeration from environmental samples in the case of bioremediation potential estimation. Tartu, 2012, 136 p.
19. **Merlin Raud.** Study of semi-specific BOD biosensors for biosensor-array. Tartu, 2013, 103 p.
20. **Ivar Zekker.** Enrichment of anaerobic ammonium oxidizing bacteria for nitrogen removal from digester effluent and anammox process acceleration by intermediate compounds. Tartu, 2013, 142 p.
21. **Annika Uibopuu.** Communities of arbuscular mycorrhizal fungi in spruce forest ecosystem and their effect on performance of forest understorey plant species. Tartu, 2013, 104 p.
22. **Jekaterina Jefimova.** Leaching of polycyclic aromatic hydrocarbons (PAHs) and heavy metals from the oil shale processing wastes and from waste-based products. Tartu, 2015, 184 p.
23. **Teele Ligi.** Bacterial community structure and its genetic potential for nitrogen removal in the soils and sediments of a created riverine wetland complex. Tartu, 2015, 127 p.
24. **Kuno Kasak.** Greenhouse gas emissions and water treatment efficiency in subsurface flow filters using various substrates. Tartu, 2016, 128 p.
25. **Martin Ligi.** Application of close range remote sensing for monitoring aquatic environment. Tartu, 2017, 146 p.
26. **Mikk Espenberg.** Impact of management on peatland microbiome and greenhouse gas emissions. Tartu, 2017, 152 p.
27. **Jens-Konrad Preem.** Forest soil bacterial community analysis using high-throughput amplicon sequencing. Tartu, 2017, 108 p.
28. **Taavi Vaasma.** Enrichment, atmospheric dispersion and deposition of naturally occurring radionuclides from oil shale-fired power plants. Tartu, 2017, 175 p.
29. **Kristjan Oopkaup.** Microbial community and its relationship with pollutant removal in treatment wetlands. Tartu, 2018, 154 p.
30. **Ergo Rikmann.** Autotrophic nitrogen removal and relevant equilibrial processes. Tartu, 2019, 179 p.

31. **Kati Klein.** Studies and treatment of inhibitory and recalcitrant wastewater. Tartu, 2021, 168 p.
32. **Thomas Schindler.** Tree stem CH₄ and N₂O fluxes in various forest ecosystems. Tartu, 2021, 182 p.
33. **Peeter Paaver.** Development of alternative binders based on oil shale fly ash. Tartu, 2021, 130 p.
34. **Kertu Tiirik.** Antibiotic resistance in connected engineered and natural aquatic environments. Tartu, 2021, 124 p.
35. **Keit Kill.** Nutrient fluxes regulation in an in-stream constructed wetland treating polluted agricultural runoff. Tartu, 2022, 144 p.